2012

FABRICATION OF AN EPITHELIAL CELL-BASED ION-SELECTIVE ELECTRODE AND ITS APPLICATION FOR USE AS ALTERNATIVE TUMOR ANGIOGENESIS ASSAY

Christina Nicole Simmons
University of Kentucky, chrissysimmons@hotmail.com

STUDENT AGREEMENT:

I represent that my thesis or dissertation and abstract are my original work. Proper attribution has been given to all outside sources. I understand that I am solely responsible for obtaining any needed copyright permissions. I have obtained and attached hereto needed written permission statements(s) from the owner(s) of each third-party copyrighted matter to be included in my work, allowing electronic distribution (if such use is not permitted by the fair use doctrine).

I hereby grant to The University of Kentucky and its agents the non-exclusive license to archive and make accessible my work in whole or in part in all forms of media, now or hereafter known. I agree that the document mentioned above may be made available immediately for worldwide access unless a preapproved embargo applies.

I retain all other ownership rights to the copyright of my work. I also retain the right to use in future works (such as articles or books) all or part of my work. I understand that I am free to register the copyright to my work.

REVIEW, APPROVAL AND ACCEPTANCE

The document mentioned above has been reviewed and accepted by the student's advisor, on behalf of the advisory committee, and by the Director of Graduate Studies (DGS), on behalf of the program; we verify that this is the final, approved version of the student's dissertation including all changes required by the advisory committee. The undersigned agree to abide by the statements above.

<div align="right">

Christina Nicole Simmons, Student

Dr. Kimberly Anderson, Major Professor

Dr. Stephen Rankin, Director of Graduate Studies

</div>

FABRICATION OF AN EPITHELIAL CELL-BASED ION-SELECTIVE
ELECTRODE AND ITS APPLICATION FOR USE AS ALTERNATIVE TUMOR
ANGIOGENESIS ASSAY

_____

THESIS

_____

A thesis submitted in partial fulfillment of the requirements for the degree of
Master of Science in Chemical Engineering in the
College of Engineering at the University of Kentucky

By

Christina Nicole Simmons

Lexington, Kentucky

Director: Dr. Kimberly Anderson, Professor of Chemical Engineering

Lexington, Kentucky

2012

ABSTRACT OF THESIS

FABRICATION OF AN EPITHELIAL CELL-BASED ION-SELECTIVE
ELECTRODE AND ITS APPLICATION FOR USE AS ALTERNATIVE TUMOR
ANGIOGENESIS ASSAY

Previous studies have provided evidence that endothelial cell-based potassium ion selective electrodes possess the ability to quantify substances that have permeability-altering effects on those endothelial cells. The capability of these so-called biosensors to detect elevated concentrations of certain chemical agents found following tumor formation make them useful in the application as an alternative tumor angiogenesis assay. In this study an epithelial cell line, human colon adenocarcinoma epithelial cells (Caco-2), was used to fabricate membranes that were used to test concentrations of these chemical agents, known as cytokines, mimicking the concentrations that have been observed in the serum of healthy individuals as well as the higher concentration found in individuals with cancer. Additionally background information is provided related to the development of whole cell-based biosensors, metabolic pathways related to tumor angiogenesis and the subsequent increase in cytokine concentration, properties of the Caco-2 cell line that make them useful for the application in cell-based biosensors, and the ultimate effect the cytokines have on the permeability of the cells.

KEYWORDS: Caco-2 Epithelial Cells, Alternative Angiogenesis Assay, Potassium Selective Electrode, Whole-Cell Based Biosensor, Cytokines

Christina Nicole Simmons

FABRICATION OF AN EPITHELIAL CELL-BASED ION-SELECTIVE
ELECTRODE AND ITS APPLICATION FOR USE AS ALTERNATIVE TUMOR
ANGIOGENESIS ASSAY

By

Christina Nicole Simmons

Dr. Kimberly Anderson
Director of Thesis

Dr. Stephen Rankin
Director of Graduate Studies

April 11, 2012

Table of Contents

List of Tables

List of Figures

Chapter 1: Introduction

1-1 Summary of Previous Work

In the recent past, whole-cell based biosensors have been used for the indirect quantification of toxins and other substances that are capable of altering cell permeability. For example, it was found that when varying concentrations of histamine were exposed to a sensor with a barrier of human umbilical vein endothelial cells (HUVECs) attached and cultured on its surface, the permeability of the cells increased, which resulted in an increased response to potassium by the potassium-selective sensor. In this way the concentration of the histamine could be determined by a linear correlation based on the response data of the cell-based potassium-selective electrode [1]. When exposed to varying concentrations of alpha toxin, the sensor returned a proportionate response to the varying concentrations of potassium ions, allowing the quantification of alpha toxin in samples by extrapolation [2]. When exposed to varying concentration of VEGF, a growth factor associated with angiogenesis during cancer, the permeability of cells increased and the sensor could be used as an indirect method for determining VEGF concentrations [3]. When exposed to cytokine solutions representative of serum of healthy individuals versus the serum of individuals with cancer, the biosensor detected a difference, thus demonstrating its potential as an alternative assay for angiogenesis [4]. By exposing this same cell-based biosensor to the actual serum of healthy individuals and individuals with varying stages of cancer, the biosensor proved to be effective in detecting a response indicative of the severity of condition of the individual [5].

1-2 Research Objectives

In previous experiments a potassium-selective cellulose triacetate membrane was used in conjunction with a specific line of endothelial cells. Studies demonstrating the *in vitro* absorption of experimental pharmaceutical chemicals utilize epithelial cells, for example T84 and Caco-2 cells because of their absorption properties have been found to be similar to the absorption properties within the human intestine. Given the extensive amounts of information available on these cells as well as their consistent and good absorption properties, the studies pertaining to the use of a biosensor as an alternative assay of angiogenesis were continued with one of these epithelial cell lines, Caco-2. In particular studies were completed to determine if a biosensor utilizing the Caco-2 cells could be used to differentiate between levels of cytokines indicative of healthy individual serum and the serum of cancerous subjects.

Chapter 2: Background

2-1 Biosensors

2-1.1 Ion-Selective Electrodes

Ion-selective electrodes are a type of analytical device used to measure the activity of specific ions in an aqueous solution. Compared to other analytical tools, the ion-selective electrode is relatively inexpensive, durable, and versatile. An additional advantage is that measurement with an ion-selective electrode is not affected by color or turbidity of the aqueous solution [6]. For measuring the change in potassium ion activity in a sample solution, a setup including an indicator electrode, a reference electrode, a transducer, and a data acquisition unit is used (Figure 2-1). As the activity of the analyte changes, the potential changes on the surface of the membrane of the indicator electrode. It is not possible to directly measure this change in potential—instead it is measured relative to the reference electrode which maintains a constant potential with respect to the sample solution [7]. The change in potential is small and a transducer is necessary to amplify the signal into something that is measureable. The transducer may be potentiometric, voltammetric, conductometric, or field-effect transistor-based [8]. For this study, a potentiometric transducer was used. The changing potential of the cell is monitored under theoretical zero current, achieved by using a high-impedance transducer.
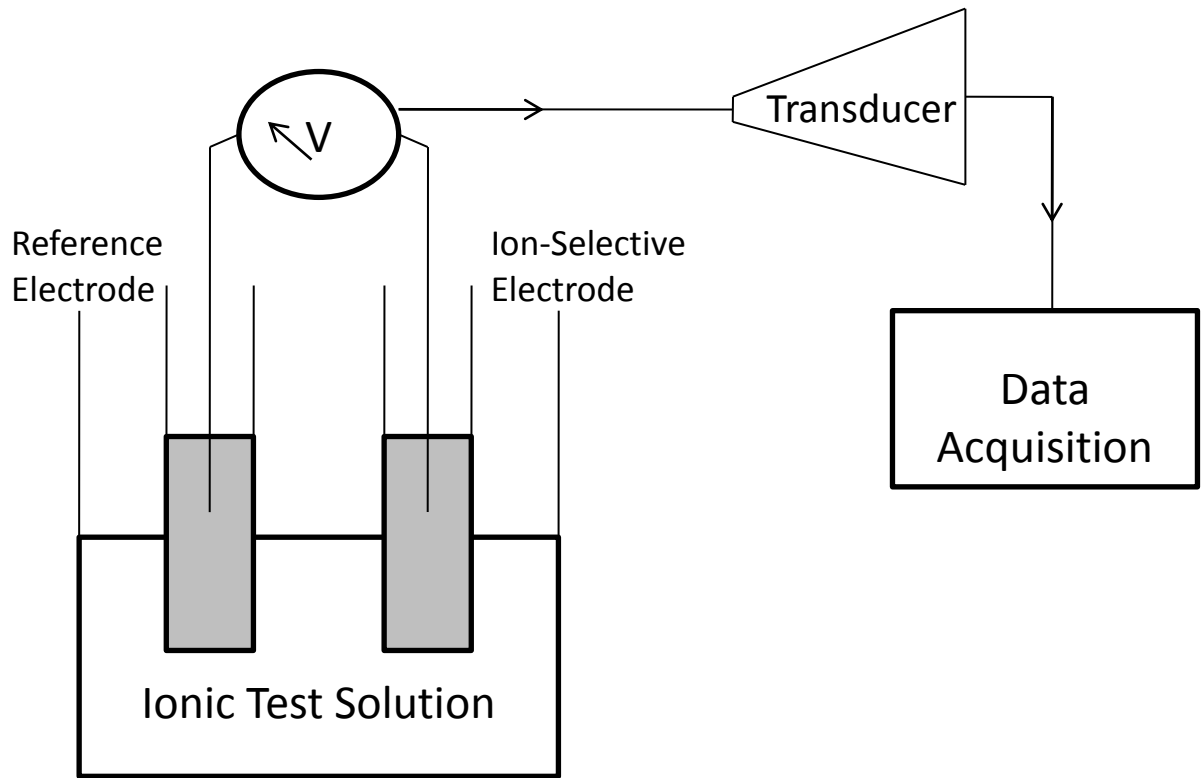
Figure 2-1: Basic setup for measuring ions with ion-selective electrode

In the ideal situation, the potential of the cell is linearly related to the logarithm of the analyte's activity, in a relationship dictated by the Nernst equation (Equation 1).

$$EMF = E^0 + \frac{RT}{zF}\ln(a_1)$$

Equation 1

EMF = electromotive force (or potential difference)

E^0 = standard cell potential

R = ideal gas constant, 8.314 J K^{-1} mol^{-1}

T = absolute temperature, 298 K

z = ionic charge of the ion of interest

F = Faraday constant, 96,485 C mol^{-1}

a_1 = activity of ion being measured

For potassium, z = 1, and Equation 1 simplifies in the following ways:

$$EMF = E^0 + 0.025678(V)\ln a_1$$

Equation 2

$$EMF = E^0 + 59.1(mV)\log a_1$$

Equation 3

The activity of a substance is related to its molar concentration according to equation 4.

$$a_1 = \gamma_1[x_1] \hspace{4cm} \text{Equation 4}$$

γ_1 = activity coefficient of species

$[x_1]$ = molar concentration of species

The potassium ion concentrations measured with the ion-selective electrode are small enough that the activity coefficient is assumed to remain constant for each concentration of potassium ions. Under this assumption, the activity is linearly proportional to the concentration. E^0 is also constant so when the concentration of potassium ions increases from $[K^+]_1$ to $[K^+]_2$, Equation 3 may be written as:

$$\Delta EMF = 59.1(mV)log\frac{[K^+]_2}{[K^+]_1} \hspace{3cm} \text{Equation 5}$$

From the data acquisition unit the change in potential may be monitored. In a calibration plot, where the cell potential is plotted against the logarithm of the concentration of potassium ions, a linear relationship is expected and the slope of the resulting line should be 59.1 mV/decade (Figure 2-2).

There are three underlying assumptions to the derivation of the Nernst Equation. First, it is assumed that only the ion of interest passes through the membrane. Second it is assumed that the concentration of the ion is appreciable at both interfaces of the membrane and also within the membrane. Finally it is assumed that no concentration gradient exists at either interface of the membrane or within the membrane [9]. Given that the three assumptions are not

perfect, a perfect Nernstian slope is not always achievable. For this study, a membrane has been classified as having a good response if it exhibits a response of 50 mV/decade or greater.

Additionally the data point for 10^{-5}M potassium consistently fell below the lower detection limit during this study, so although the EMF of that point was always recorded, it was not factored into the calculation of the slope. Figure 2-3 is a good example of an actual data set that demonstrates typical behavior of these membranes. Two possible explanations exist to elucidate why membranes may deviate from Nernstian behavior at low concentrations. One is that the membrane loses a small concentration of potassium ions which cancels out the effect of any influx of potassium ions from the sample solution. The second possibility is that interfering ions affect the transport of potassium ions through the membrane and such interference is exaggerated at low concentrations of potassium ions [10].
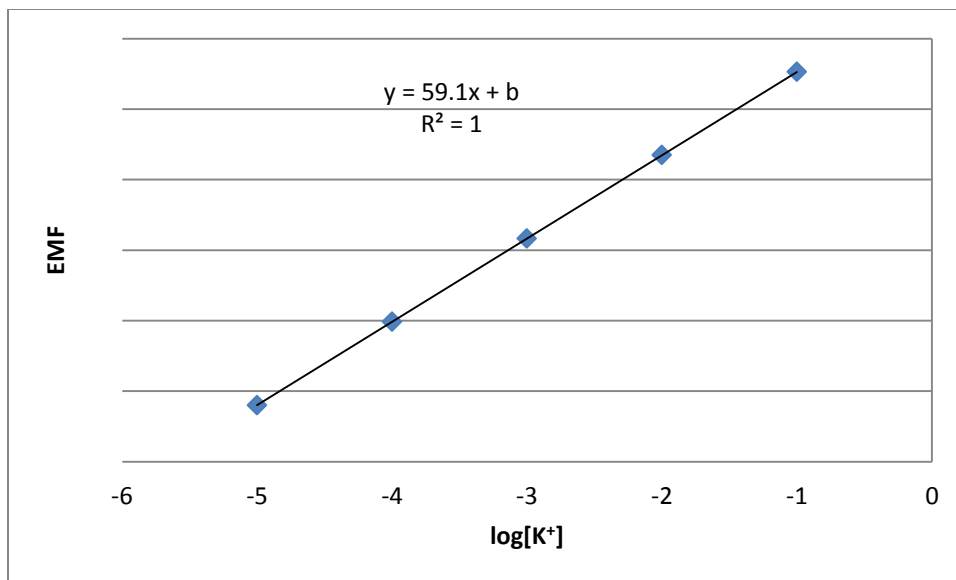
Figure 2-2: Expected calibration curve exhibiting Nernstian behavior
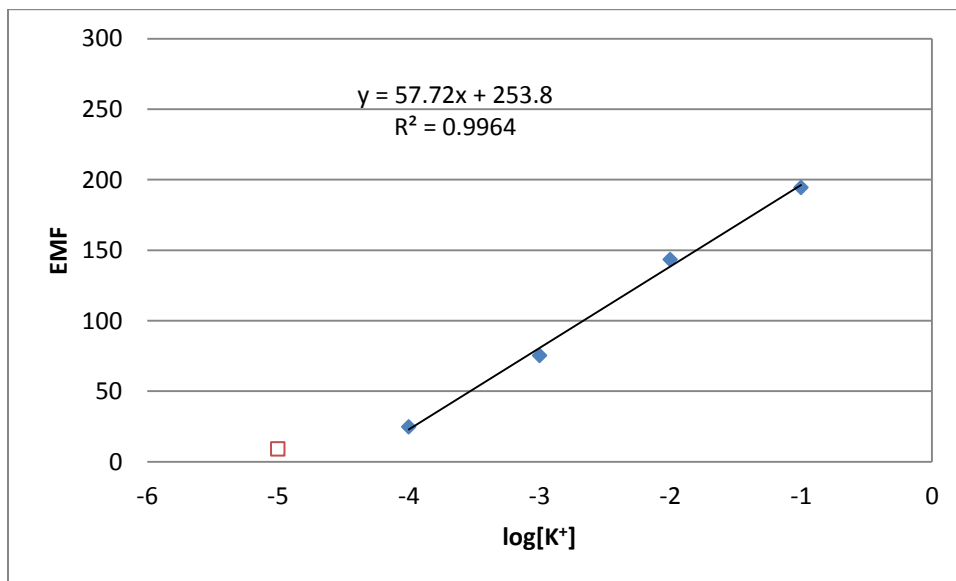
Figure 2-3: Sample calibration curve exhibiting actual data from fabricated membrane #32, section "C", identified as 32(C)

2-1.2 Ion-Selective Membranes

The final membrane that will be used here is composed of cellulose triacetate, potassium tetrakis[3,5-bis(trifluoromethyl)phenyl]borate (KTTFPB), valinomycin, and 2-nitrophenyl octyl ether (NPOE) and its purpose is to selectively detect potassium ions. The membrane is asymmetric—it is composed of two layers with different compositions. The first layer, which is ultimately in contact with the analyte solution, is composed of the polymer while the second layer contains the polymer and the active components that are responsible for ion detection. Although the second layer on its own is sufficient for selectively monitoring potassium ions, the first layer is present so that the bioreagents may be attached covalently to the surface of the membrane after the first layer is hydrolyzed [11].

Cellulose triacetate (CTA) was used as the polymer matrix of the membrane. The goal of the biosensor is ultimately to detect toxins in physiological samples, so formation of an electrode that is biocompatible is important. Fibrin formation and clotting have been observed in polyvinyl chloride (PVC) membranes used in whole blood samples. One method for reducing such undesirable behavior in blood samples is to attach heparin to the electrode's membrane. It has been documented that heparin attachment is more readily achieved on a CTA-based membrane when compared to a PVC-based membrane [12]. Because it is possible to achieve desirable electrode response whether CTA or PVC is used for the membrane's polymer matrix, cellulose

9

triacetate is considered to be more ideal than PVC due to its potentially increased biocompatibility applications.

Valinomycin is used in the membrane to facilitate transport of the potassium across the membrane. Valinomycin is a neutral-carrier ionophore produced by the bacteria *Streptomyces fulvissimus*. The structure of valinomycin is a macrocyclic ring, composed of 12 alternating amino acids and hydroxy acids. For clinical analysis of potassium concentration, valinomycin is the most commonly used ionophore [13]. The frequent use of valinomycin is due to its high selectivity for potassium in comparison to other monovalent cations. In fact the stability constant between valinomycin and potassium exceeds that of valinomycin and sodium by a magnitude of 10^5 [14]. It forms a complex with potassium ions when the oxygen from 6 of its carbonyl groups surrounds a single potassium ion. Its large macrocyclic structure allows it to remain conformationally flexible even after complexation with a potassium ion. This flexibility allows the valinomycin to quickly bind with the potassium ion at one interface of the membrane and quickly release the potassium ion at the opposite interface of the membrane [15].

Potassium tetrakis[3,5-bis(trifluoromethyl)phenyl]borate (KTFFPB) is used to give the ion-selective membrane anionic sites necessary to exclude the counterion that may compete with the cation of interest for detection [10]. Addition of the salt increases the membrane's selectivity for potassium ions, decreases the electrical resistance of the membrane, and decreases the

response time of the electrode [16]. Figure 2-4 illustrates the formation of the valinomycin-potassium complex and also the added anionic exchanger sites.

The final component of the membrane is a plasticizer. To ensure sufficient ionic conductivity, it is necessary that the glass transition of the membrane be lower than room temperature [17]. The glass transition temperature (T_g) of CTA is 185.8 °C. A plasticizer, in this case NPOE, is required to make the membrane more fluid.
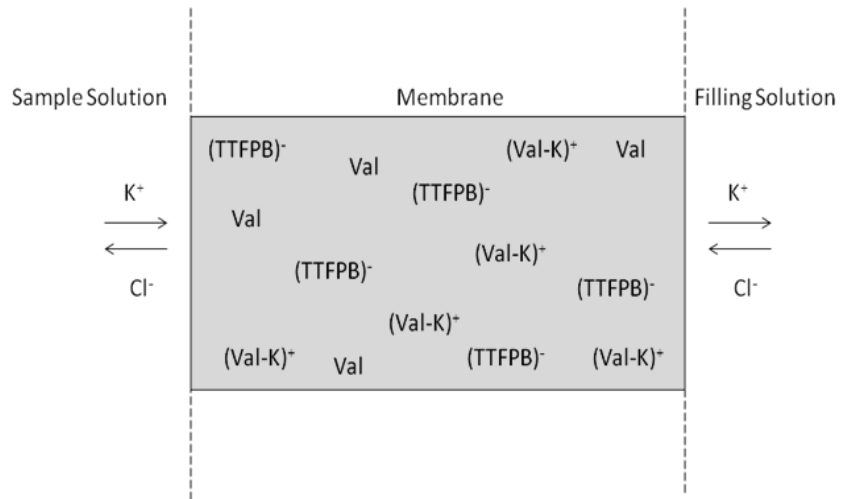
Figure 2-4: Schematic of ionophore-cation complex and anionic exchanger sites in the membrane (adapted from [17])

2-1.3 Utilizing Cells as Recognition Element

The ion-selective membrane used in the ion-selective electrodes may be combined with some biological material to create a biosensor able to detect the presence of other biologically significant substances. In previous studies human endothelial vein cells (HUVECs) were used as the biological material [1-5]. Because a confluent layer of cells is nearly impermeable to many ions, growing cells onto the surface of an ion-selective electrode renders the electrode unresponsive to the ions. When permeability-modifying substances are exposed to a confluent cell layer, the cells become more permeable and allow ions to pass through the cell layer via a few known existing mechanisms which will be discussed later in this paper. The electrode becomes more responsive in proportion to the change in the permeability of the cells, which is itself proportional to the amount of the permeability-modifying agent that was exposed to the cell layer as well as the amount of time it was exposed. By maintaining constant exposure times, the amount of permeability-modifying substance that is present in a sample is proportional to how responsive the ion-selective electrode is to the ions.

2-1.4 Cell Adhesion to Synthetic Membranes

In order to attach cells to the membrane, some chemical modifications must be made to the membrane's surface. The ester group of the cellulose triacetate is hydrolyzed under basic conditions with sodium hydroxide (NaOH) to add hydroxyl groups under a saponification reaction (Figure 2-5). Next a second layer containing the anion-repelling salt, the ionophore, and the plasticizer is

added to the untreated side of the membrane, and then the treated side of the first layer is exposed to a surface active agent, CDI, or carbonyldiimidazole (Figure 2-6). This allows RGD (Arginine-Glycine-Aspartic Acid) to be immobilized on the surface of the CTA membrane via the amide bond, and finally the cells are attached to the surface of the membrane through an interaction between the extracellular matrix and the peptide sequence (Figure 2-7).
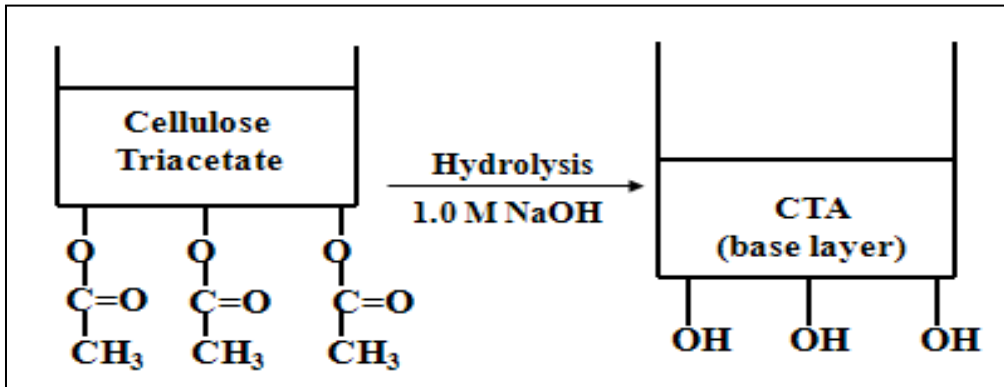
Figure 2-5: Ester group is hydrolyzed with sodium hydroxide to add hydroxyl groups under a saponification reaction (adapted from [1])
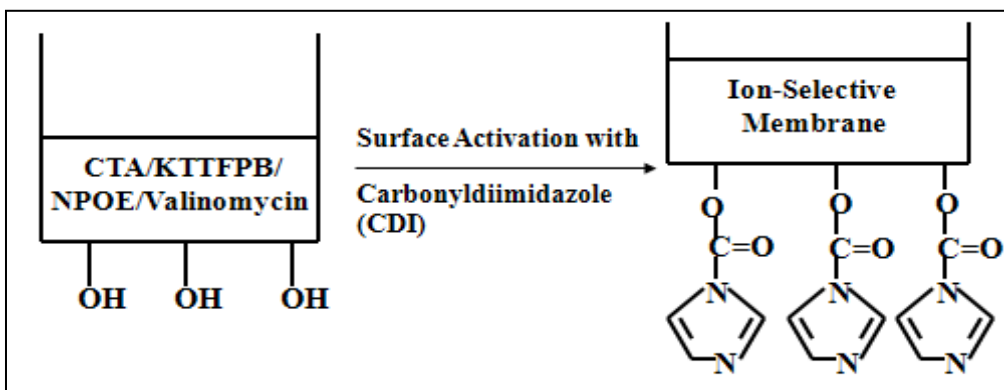
Figure 2-6: Addition of a second layer to the membrane and the hydrolyzed side of membrane is exposed to a surface active agent (adapted from [1])
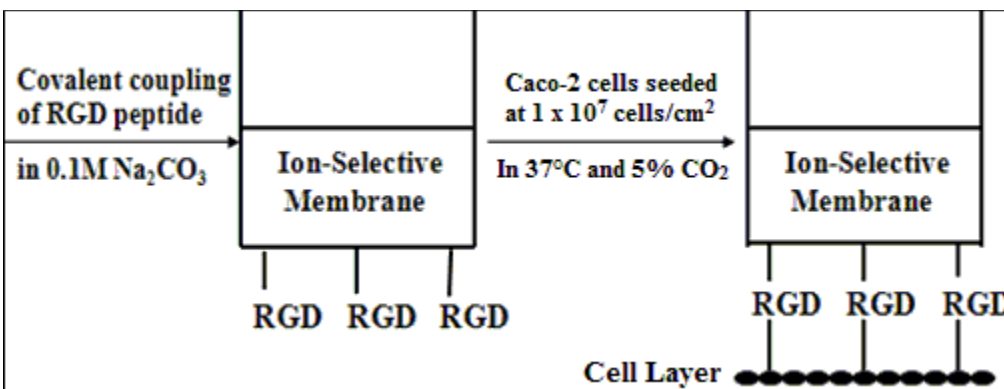
Figure 2-7: RGD is immobilized on the surface of the CTA membrane via the amide bond and cells are attached to surface of the membrane through the RGD peptide sequence (adapted from [1])

2-2 Caco-2 Cells

2-2.1 Differentiation and Proliferation

The morphology of Caco-2 cells makes them an attractive candidate for modeling the absorption of pharmaceutical chemicals by *in vitro* methods. Seven days after seeding Caco-2 cells at a cell density of 6×10^4 cells/cm^2, a monolayer of poorly differentiated cells is formed, which is confirmed by a lack of tetramethylrhodamine (TRITC)-phalloidin staining of filamentous actin (F-actin) fibers. By day 21, the cells are columnar in shape and are more strongly differentiated with a well-established brush border and by day 28 the cells reach a maximum level of confluency [18]. Caco-2 cells form structures similar to intestinal enterocytes, which allows the cells to be used as a model for mimicking the absorption of candidate oral pharmaceutical drugs through the human intestine [19-21].

Although using Caco-2 cells is popular for the *in vitro* modeling of intestinal absorption, one disadvantage to their use are the lengthy culture times required for the cells to mature and form tight, nearly impenetrable monolayers. Allowing the cells to fully develop into useful, well-matured monolayers generally take approximately 3 weeks. Some examples follow:

When testing the permeability-altering effects of elevated glucose concentrations on Caco-2 cells, the cells were seeded with a density of 2.5×10^5 cells/well (5.3×10^4 cells/cm^2) and grown for a minimum of 21 days [22]. To evaluate the *in vitro* bioabsorption of aloe components, cells were seeded on transwell polyester membrane filters with a density of 6.4×10^6 cells/cm^2 and were used in tests 14-21 days after the cells formed a confluent monolayer [23].

After Caco-2 cells were seeded onto transwell clear polyester membranes with a seeding density of 1 x 10^5 cells/cm^2, the cells were reported to reach confluency within 3-4 days and were used 21-25 days to test the uptake and transport properties of propranolol [24]. Caco-2 cells were seeded in transwell plates with a density of 8 x 10^4 cell/cm^2 and allowed to differentiate for 25 days before use in experiment to determine the effect of acetaldehyde on paracellular drug permeability [25].

BD Biosciences (San Jose, CA) has created a method that it claims is capable of creating fully differentiated Caco-2 cell monolayers in only 3 days following seeding. Its system includes specialized collagen-coated substrates, serum-free media, and cell-seeding density of 4.65 x 10^5 cells/cm^2. While the Caco-2 cell monolayers have been tested using this method and found to form a sufficient barrier for testing permeability, leakier cell monolayers were observed when compared to traditional 3 week Caco-2 permeability studies [26].

Other approaches to developing Caco-2 cell monolayers capable of rapid maturation and differentiation involve determining the most suitable range for passage numbers. At higher passage numbers, Caco-2 cells demonstrate an increased expression of P-glycoprotein (P-gp) protein, a cellular efflux pump, which results in greater accuracy and repeatability of permeability studies [27]. In Caco-2 cells P-glycoprotein acts as a deterrent to the absorption of solutes. It is present in the monolayer of Caco-2 cells but is not uniformly expressed. The level of expression in the monolayer of cells determines how permeable the cell layer is [28].

2-2.2 Predicting Intestinal Absorption

After the cells have reached a suitable level of proliferation and differentiation, there are a variety of ways to test the integrity of the monolayer. One common method involves using a marker molecule, for example [^{14}C]mannitol, which is allowed to passively diffuse across the barrier of cells, and the number of marker molecules that pass through are counted by liquid scintillation spectroscopy [29-33]. A similar method may be employed with fluorescent labeled marker molecules and quantified using a fluorescent spectrophotometer or fluorescent microscopy [33-36]. Perhaps the most common method for evaluating the barrier properties of the cell monolayer is by measuring the transepithelial electrical resistance, or TEER [30-32, 34-36]. To measure the TEER, cells are grown on filters in a specialized unit. One electrode of a resistance meter is inserted in the apical chamber and one electrode is inserted in the basolateral chamber. As the cell monolayer becomes more differentiated, the passive diffusion of ions between the chambers slows which results in an increase in the resistance across the cell layer [37].

2-3 Angiogenesis
2-3.1 Angiogenic Switch

Tumor cells face hypoxia when rapid cell proliferation results in the diameter of the tumor exceeding oxygen's diffusion limit for transport from capillary blood vessels to cells. Under these circumstances the tumor is able to sustain its growth by forming new, farther-reaching blood vessels, in a process called angiogenesis. Vital to this activation of the "angiogenic switch" is a

transcriptional factor known as hypoxia-inducible factor (HIF-1), a heterodimer, consisting of alpha and beta subunits. Under normoxic conditions, or when oxygen concentrations are normal, the proline residue on HIF-1α is hydroxylated. In addition to oxygen, this reaction requires iron, α-Ketoglutarate, and ascorbic acid. The product resulting from the expression of Von Hippel-Lindau (VHL) gene, Von Hippel-Lindau Protein, or pVHL, plays a role in the management of angiogenesis. The prolyl hydroxylation results in the stabilization of HIF-1α, allowing pVHL to bind to it. While HIF-1α is present in all cell types under normoxic conditions, it is usually not detectable unless the cells are exposed to hypoxic conditions and then rapid accumulation of HIF-1α is observed with time [38].

2-3.2 Production of Cytokines

This research focuses on the permeability-altering effects of 4 particular cytokines:

- Vascular endothelial growth factor (VEGF)

- Hepatocyte growth factor (HGF)

- Basic fibroblast growth factor (bFGF)

- Tumor necrosis factor alpha (TNF-α)

Under hypoxic conditions, the concentrations of all four of these cytokines of interest are increased in serum by a few chemical pathways. Following the angiogenic switch, HIF-1α increases the expression of VEGF [39], HGF [40], and bFGF [41]. HIF-1α does not appear to be responsible for the accumulation of

19

TNF-α during hypoxia. Instead TNF-α expression is increased by the transcription factor, Nuclear Factor Kappa B (NF-κB) after it is activated during hypoxic conditions [42, 43]. The approximate concentrations of the cytokines found in the serum of healthy subjects as well as subjects with cancer are summarized in Table 2-1. It has been assumed that each of the cytokines of interest would have a combined effect in an actual physiological environment, which would result in a more dramatic effect on Caco-2 cells when compared to isolated cytokines in a solution. For this reason, the tests done during this study used elevated levels of cytokines to inflate the effects that the individual cytokines would have on the response of the cells. These elevated levels are summarized in Table 2-2.

Table 2-1: Mean Cytokine Concentrations Observed in the Serum of Healthy Subjects and Subjects with Cancer

	Serum of Healthy Subjects Levels (pg/ml)	*Serum of Subjects with Cancer Levels (pg/ml)*
VEGF	**122.8 – 201.7** [44]	**331.5 – 831.4** [44-46] *mean = 331.5, 360.0, 295.7, 833.4 (Stage I, II, III, and IV breast cancer, respectively)* [44] *479 ± 461 (metastatic colorectal, breast, ovarian, renal carcinoma)* [45] *564.5 ± 147.88 (breast carcinoma)* [46]
bFGF	**0 – 4.93** [47]	**6.64 – 11.4** [45, 47] *11.4 ± 10.6 (metastatic colorectal, breast, ovarian, renal carcinoma)* [45] *mean = 6.64 (prostatic carcinoma)* [47]
HGF	**343.00** [48]	**529.05** [48] *529.05 ± 123.33 (breast carcinoma)* [48]
TNF-α	**5.2** [46]	**28.6** [46] *28.6 ± 7.99 (breast carcinoma)* [46]

Table 2-2: Cytokine Concentrations Used in this Experiment to Represent Normal Levels of Cytokines and Elevated Levels of Cytokines

	Serum of Healthy Subjects Levels (pg/ml)	*Serum of Subjects with Cancer Levels (pg/ml)*
VEGF	100	1000
bFGF	5	40
HGF	100	1000
TNF-α	10	100

2-3.3 Cytokine Effects on Cell Permeability

The cytokines related to angiogenesis affect the permeability of Caco-2 cells, as well as other epithelial cells, by inducing changes in the morphology of the structures that join neighboring cells. Between the cells in a layer are 3 types of cell junctions:

- Adherens junctions

- Gap junctions

- Tight junctions

Adherens junctions composed of two different types of proteins: cadherins and catenins. Cadherins are calcium-dependent cell adhesion molecules that are linked to the cytoskeleton of cell through catenins. There are various types of cadherins and they are named according to where they are located. For example, cadherin located in retinal cells is referred to as R-cadherin, while the cadherin found in epithelial cells is called E-cadherin.

Gap junctions are cell junctions that are specialized for intercellular communication. They are composed of one type of protein: connexin. Connexins are made of 6 subunits arranged around an annulus. Gap junctions are gated—at least one of the connexin's subunits is believed to close the junctions in situations when certain ions become elevated within the cells.

Tight junctions are located between adjacent epithelial cells, apically relative to the rest of the cell junctions of the junctional complex. Tight junctions are composed of two different types of proteins: occludins and claudins. The strength of the adhesion between the cells via tight junctions is related to the type

of these proteins within the tight junctions. Occludin is composed of two peptide sequence loops which are responsible for the tight junctions' adhesive properties. The effectiveness of the barrier between cells is compromised when a synthetic peptide sequence mimicking one of these loops is introduced to a cell layer [49]. Additionally, when occludin is expressed in Madin-Darby Canine Kidney (MDCK) cells, the integrity of the cell monolayer is improved [50].

It has been shown that the phosphorylation of certain proteins in the junctional complex can lead to the reduction of the adhesive properties between cells [51-53]. When exposed to HGF MDCK cells developed newly phosphorylated E-cadherin [54]. When Caco-2 cells were exposed to TNF-α, the occludin protein became more phosphorylated, resulting in the observation of the decrease in the transepithelial resistance between the cells. In fact after exposing the cells to TNF-α, a change in morphology between the cells was observed, including a reduction in the number of tight junctions as well as enlarged spacing between the cells [55]. It has been demonstrated that VEGF phosphorylates connexin 43 in the gap junctions of a human umbilical vein cell line's (Ea.hy926) cells [56]. Downregulation of cadherins has been observed in the presence of bFGF in HUVEC cells [57].

Changes in the cell junction morphology cause changes to the paracellular permeability of the cells. Altering the cell junctions allow solutes to pass between neighboring cells, driven by passive diffusion from higher concentrations to lower concentrations. In this research 2 sets of experiments were performed. In the first experiment, the cytokines' effects on paracellular

gap area were tested and the impact on paracellular permeability was explored. In the second experiment, the effects of the cytokines on the responsiveness of a cell-based electrode were tested and changes were expected via a combination of each pathway. Figure 2-8 illustrates the difference between these two pathways.
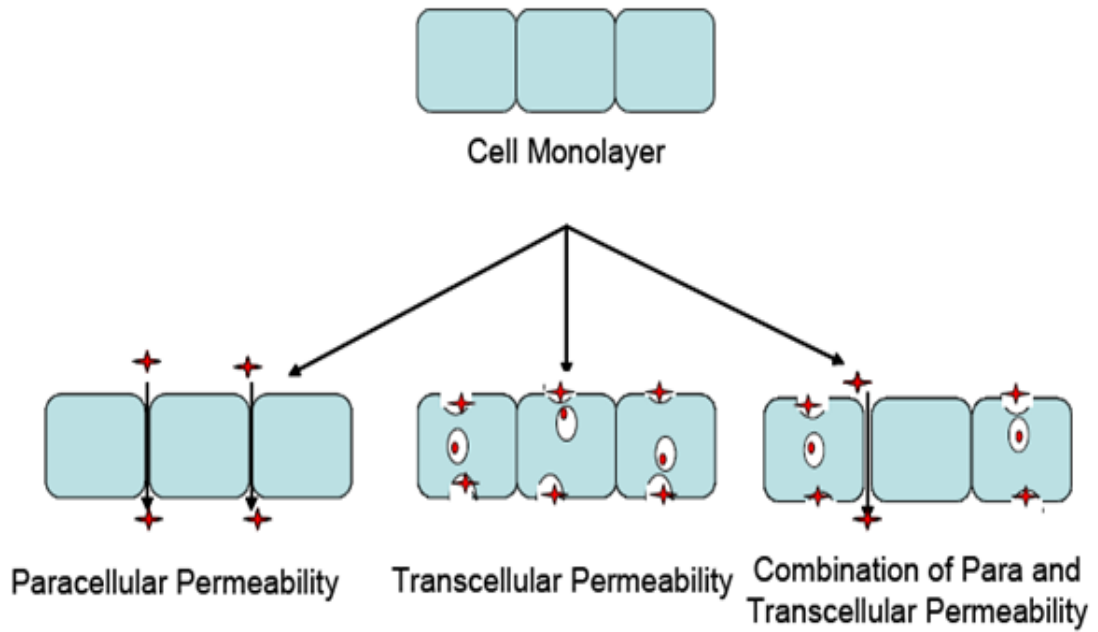
Figure 2-8: Demonstration of two main pathways for solutes to travel across a cell monolayer [58]

Chapter 3: Experimental Materials

3-1 Membrane Fabrication

Celluose triacetate (Cat. # 181005), Selectophore™ grade Tetrakis[3,5-bis(trifluoromethyl)phenyl]boron potassium (Cat. # 60588), Selectophore™ grade Valinomycin (Cat. # V0627), Selectophore™, grade, ≥99.0% 2-Nitrophenyl octyl ether (Cat. # 73732), CHROMASOLV®, grade for HPLC, ≥99.8% Chloroform (Cat. # 366927), reagent grade, ≥98.0% Tetrachloroethane (Cat. # 185434), ACS reagent, ≥99.5% Dichlormethane (Cat. # D65100), and reagent grade, ≥98% Sodium hydroxide pellets (Cat. # S5881) were obtained from Sigma-Aldrich (St. Louis, MO).

3-2 Testing Membranes

≥99.0% Potassium chloride (Cat. # P5405), reagent grade, ≥99.0% (titration) Trizma® hydrochloride (T3253), and ≥99.9% (titration) Trizma® base (T1503) were obtained from Sigma-Aldrich (St. Louis, MO).

3-3 Treatment of Caco-2 Cells

3-3.1 Culturing Caco-2 Cells

Caco-2 cells at passage 20 (Cat. # HTB-37), Fetal Bovine Serum, or FBS, (Cat. # 30-2020), and Eagle's Minimum Essential Medium (Cat. # 30-2003) were obtained from American Type Culture Collection (ATCC, Manassas, VA). The medium contained Earles Balanced Salt Solution, non-essential amino acids, 2 mM L-glutamine, 1 mM sodium pyruvate, and 1500 mg/L sodium bicarbonate and was supplemented with Fetal Bovine Serum to a final concentration of 20%.

3-3.2 Subculturing Caco-2 Cells

Trypsin Ethylenediaminetetraacetic Acid, or Trypsin-EDTA, (0.25%-0.53mM) in Hanks Balanced Salt Solution was obtained from American Type Culture Collection (Manassas, VA).

3-3.3 Attaching Caco-2 Cells to Membrane

Glycine-Arginine-Glycine-Aspartic Acid-Serine (GRGDS) (Cat. # H-1345) was obtained from Bachem (Torrance, CA). ≥99.85% Glacial acetic acid (Cat. # 695084), *ReagentPlus*® grade, ≥99.5% Sodium carbonate (Cat. # S-2127), 99.5-100.5% Sodium bicarbonate (Cat. # S-5761), *ReagentPlus*® grade, ≥99.0% Sodium acetate trihydrate (Cat. # S-8625), and ≥97.0% (T) 1,1′-Carbonyldiimidazole (Cat. # 21860) were obtained from Sigma-Aldrich (St. Louis, MO).

3-3.4 Permeability Studies

Carrier-free recombinant human VEGF165 (Cat. # 293-VE-010/CF), HGF (Cat. # 294-HGN-005/CF), TNF-α (Cat. # 210-TA-010/CF), bFGF (Cat. # 233-FB-025/CF) were obtained from R&D Systems (Minneapolis, MN).

3-3.5 Freezing Caco-2 Cells for Storage

Hybri-Max™ grade, ≥99.7% filter-sterilized Dimethyl sulfoxide, DMSO, (Cat. # D2650) was obtained from Sigma-Aldrich (St. Louis, MO).

Chapter 4: Experimental Methods

4-1 Membrane Fabrication

To make the cocktail for the 1st layer of the membrane, 74 $\pm$ 0.2 mg of Cellulose triacetate was dissolved overnight at ambient conditions in 1.1 ml of dichloromethane, 0.4 ml of chloroform, and 0.4 ml of tetrachlorethane. To form a seal to prevent leakage, approximately 0.5 ml of the 1st layer cocktail was applied around the inner edge of a 31 mm ID glass ring resting on a piece of Teflon. After approximately 1 minute, the remainder of the 1st layer cocktail was added to the 31 mm ID glass ring.   A Teflon plate was placed on top of the glass ring and the solvents were allowed to evaporate for at least 48 hours through venting grooves cut into the glass ring. After the solvents evaporated, the membrane was removed from the glass ring and the side formerly in contact with Teflon was hydrolyzed in 1.0M NaOH for 4.5 hours.   During the casting process, the membrane formed raised edges and this ensured that only one surface of the membrane contacted the NaOH. After hydrolysis, the membrane was rinsed thoroughly with DI Water, patted dry with a KimWipe, and placed hydrolyzed-side down on a piece of Teflon. A 25 mm ID glass ring was placed in the center of the membrane and the 1st layer was allowed to dry completely overnight.

To make the cocktail for the 2nd layer of the membrane, 34 $\pm$ 0.1 mg of Cellulose triacetate, 1 mg of Valinomycin, 0.42 mg of KTTFPB were dissolved overnight at ambient conditions in 0.8 ml of dichloromethane, 0.8 ml of chloroform, and 0.1 ml of NPOE.   To form a seal to prevent leakage, approximately 0.5 ml of the 2nd layer cocktail was applied around the inner edge

of the 25 mm ID glass ring resting on the 1st layer of the membrane. After approximately 1 minute, the remainder of the 2nd layer cocktail was added to the 25 mm ID glass ring. The solvents were allowed two days to dry from the second layer and the second layer fused with the first layer to form a single asymmetric membrane.

4-2 Testing Membranes

Each membrane was sectioned into five 6 mm discs using a cork borer. One section per each fabricated membrane was used as the control to determine how other membrane sections would respond before cells were grown on a section's surface. The membrane section was conditioned in 0.01M potassium chloride (KCl) after it was placed in a membrane housing piece in an orientation so that the hydrolyzed surface was in contact with the conditioning solution. The membrane was conditioned for 24 hours in the KCl solution0 to allow an equilibrium to establish within the membrane. Then the membrane housing piece was attached to an electrode body with 0.01M KCl filling solution. The electrode, along with a reference electrode, was placed in 50 ml of 0.1M Tris(hydroxymethyl) aminomethane (Tris) buffer that was stirred slowly with a stir bar. To the sample solution, the following quantities of KCl were serially added: 5 μl of 0.1M KCl, 50 μl of 0.1M KCl, 50 μl of 1.0M KCl, 500 μl of 1.0M KCl, and 5.6 ml of 1.0M KCl. These additions changed the potassium concentration of the sample solution from 0M to 10^{-5}M, 10^{-4}M 10^{-3}M, 10^{-2}M, and 10^{-1}M and the EMF was recorded at each concentration. A plot was made of the EMF vs. the logarithm of the potassium concentration and the slope was calculated for the

last 4 data points. If the slope was greater than 50 mV/decade, then the membrane's performance was considered to be sufficiently responsive and small sections of the membrane was saved for use in further tests.

4-3 Treatment of Caco-2 Cells

4-3.1 Culturing Caco-2 Cells

Upon receipt, the cryovial containing the frozen Caco-2 cells was rapidly thawed by submersion in a water bath maintained at 37°C. Under a sterile laminar flow hood, the contents of the vial were transferred to a 15 ml centrifuge tube containing 9 ml of complete culture medium. The cells were spun down in a centrifuge for 5 minutes and the supernatant was discarded. The cells were resuspended in 15 ml of complete medium and transferred to a 75 cm^2 culture flask with a vented cap. The cells were incubated at 37°C in 5% CO_2. The media was replenished twice per week until the cells formed a confluent monolayer on the surface of the culture flask.

4-3.2 Subculturing Caco-2 Cells

After the cells reach confluency, the media of the culture flask was discarded. 20 ml of heat-sterilized phosphate buffered saline (PBS) solution was added to the flask and incubated at 37°C for 4 minutes to remove serum and Ca^{2+} that inhibit the Trypsin-EDTA. The sterile PBS solution was then removed and discarded and 5 ml of Trypsin-EDTA was added to the flask. The flask was incubated at 37°C for 15 minutes or until the cell layer detached from the culture flask. 7 ml of complete growth medium was added to the culture flask and the cells were gently aspirated by pipetting. The cell solution was divided equally

into four 15 ml centrifuge tubes and spun down in a centrifuge with a swing-out rotor assembly for 5 minutes. The supernatant was removed and discarded and the cells were cultured in a new flask or well plates, attached to test membranes for experimentation, or added to freezing solution for storage in liquid nitrogen.

4-3.3 Counting Caco-2 Cells

Cell counts were performed using a hemocytometer. First the media was removed from the stationary flask and discarded. Next the cells were rinsed with 10 ml PBS to remove any residual serum. Then the cells were exposed to 9 ml of Trypsin-EDTA to detach the cells from the flask. The cell solution was split into 3 centrifuge tubes and spun down to separate the Trypsin-EDTA from the cell pellet. The Trypsin-EDTA was removed with a pipette and discarded. To the centrifuge tubes 45 ml of growth media was added and the cells were mixed thoroughly by gentle aspiration with a pipette. The cell solution was further diluted by withdrawing 1 ml of dilute cell solution and adding it to 3 ml of growth media. A couple of drops of this solution were added to a hemocytometer, so that the face was completely flooded. Under a microscope with a 10x exposure, the numbers of cells within the boxes depicted in white in Figure 4-1 were counted and the average per square grid was taken. An image of one square grid with cells is shown in Figure 4-2. The number of cells per volume of original mixture could be calculated from Equation 7.

$$C = \left(\frac{X_A}{V_g}\right)\left(\frac{V_D}{V_S}\right)$$

Equation 7

where:

$C = concentration\ of\ cells\ in\ original\ mixture\ (\#/ml)$

$X_A = average\ number\ of\ cells\ per\ square\ grid$
$V_g = (volume\ of\ one\ square\ grid) = 10^{-4}\ ml$

$$\left(\frac{V_D}{V_S}\right) = \frac{volume\ of\ sample\ dilution}{volume\ of\ original\ mixture\ in\ sample} = 180$$
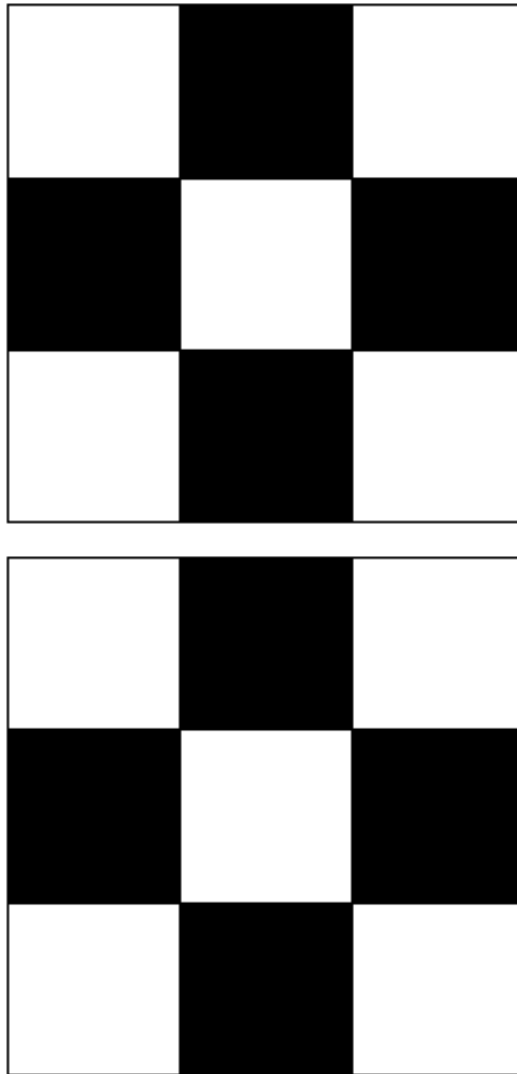
Figure 4-1: Schematic of square grids of a hemocytometer. The white squares represent the area where cells were counted.
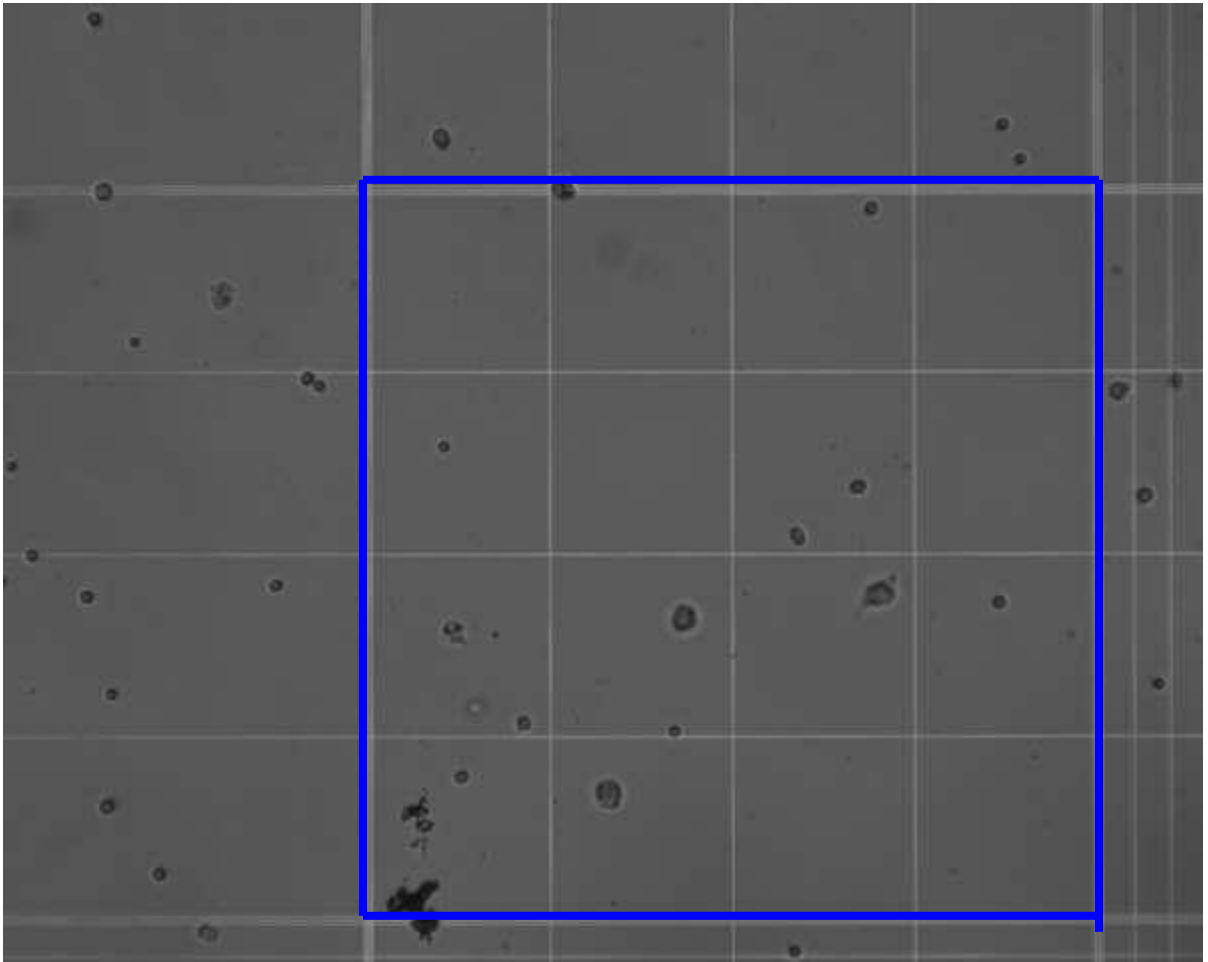
Figure 4-2: 10x microscope image of a single square grid of hemocytometer loaded with Caco-2 cells.

4-3.4 Attaching Caco-2 Cells to Membrane

Up to five 6 mm discs may be obtained from the membrane. After the control membrane was confirmed to perform satisfactorily, four more sections were cut from the membrane. Before the sections could be cut, they needed to be prepared for cell attachment. The remaining untested portion of the membrane was floated in 20 ml of refrigerated DI water with the hydrolyzed side in contact with the water. Approximately 0.34 g of carbonyldiimidazole was added to the beaker in five increments of 3 minutes. The membrane was then rinsed with refrigerated DI water and floated in a 50-ml glass beaker containing 3 ml of 0.1M sodium carbonate and 1.5 mg of GRGDS peptide. The beaker was placed in an incubator shaker set at 25°C and 100 rpm for approximately 24 hours. Afterwards, the membrane was rinsed for a few minutes in 0.1M sodium bicarbonate followed by a brief submersion in DI water. It was then rinsed for a few minutes in 0.1M sodium acetate that has been adjusted to pH 4 with acetic acid. It was again submerged briefly in DI water and then left under a UV light in a hood to be sterilized overnight. The following day the remaining sections of the membrane were cut using the cork borer and placed in the membrane housing pieces. The membrane sections were then conditioned for 24 hours in 0.1M KCl that has been sterilized by autoclaving.

The cells, which have reached confluency in the culture flask by this point, were split into 3 centrifuge tubes, counted using a hemocytometer, and then diluted to a final concentration of approximately 4.7×10^6 cells/ml. 2 ml of the diluted cell suspension is added directly to the surface of the membrane, which is

still in the membrane housing piece. The membrane housing piece is then placed in an incubator for 72 hours while the cells grow into a confluent layer on the membrane's surface.

4-3.5 Freezing Caco-2 Cells for Storage

Between experiments, the unused Caco-2 cells were frozen and stored for use in future tests. In order to freeze the Caco-2 cells for storage, a mixture consisting of 95% complete growth medium and 5% filter-sterilized DMSO was made. The cells in a stationary flask were split into 3 centrifuge tubes, using the previously described method for subculturing the cells. To each centrifuge tube, 2 ml of freezing solution was added and each centrifuge tube was split into 2 cryovials. The cryovials were frozen overnight at -80°C and then stored in a cryotank of liquid nitrogen.

4-4 Testing Permeability Effects of Cytokines
4-4.1 Paracellular Gap Area

The method for determining the area resided by cells using computer-assisted image analysis has been briefly outlined [59].

In 24 well plates Caco-2 cells were cultured until they reached confluency. The media was disposed and each well was rinsed with 2 ml of sterile PBS. After shaking, the PBS solution was removed from each well and disposed of. The cells were exposed to the various test agents and incubated at 37°C for 1 and 3 hours. Following incubation, the test agent was removed from each well and discarded. To each well, 1 ml of 3% paraformaldehyde (PFA) was added to the cells and the cells were fixed under a sterile laminar flow hood at ambient

conditions for 30 minutes. The cells were rinsed with 2 ml of sterile PBS two additional times. The cells were stained with Coomassie blue solution for 10 minutes. The cells were rinsed with sterile PBS solution multiple times until the excess dye was removed and the discarded PBS was clear in color. The cells were allowed to dry under ambient conditions for approximately 30 minutes.

Images were captured of each well plate under an inverted phase contrast microscope at 320x and 50 ms exposure time using AxioVision4. All images were converted to Tagged Image File Format (Tiff) files and analyzed with Scion Image. Upon 16x magnification, the threshold pixel was selected to correspond to the area just outside the edge of an individual cell. The image was then converted to a binary image and the image was inverted, so that the white pixels corresponded to the gaps and the black images corresponded to the cells. A histogram was given for each selection and from that histogram, the number of white pixels as well as the total number of pixels could be determined. The paracellular gap area was then expressed as a ratio of the number of white pixels to the total number of pixel values in a given selection (Equation 8).

$$\% \, Paracellular \, Gap \, Area = \frac{\# \, of \, White \, Pixels}{Total \, Sum \, of \, Pixel \, Values} \, x \, 100\% \qquad \text{Equation 8}$$

For each image, 4 selections were made for calculating 4 different paracellular gap areas per each well.

4-4.2 Electrode Response

After 3 days of incubation, the inhibition of response of the electrode is tested to ensure the cells have formed a confluent layer on its surface. After each addition of KCl, the EMF value is recorded. The ion-selective electrode response slope is the slope of these EMF values versus the logarithmic molarity of potassium. The ion-selective electrode response of the test membrane is divided by the ion-selective electrode response of the control membrane to give a ratio. In the past a ratio of approximately 0.05 was observed for the response of electrodes with a confluent layer of cells when compared to the response of an electrode without cells. A ratio equal to or less than 0.05 was considered to be indicative of a well-developed cell layer on the surface of the electrode. Each time cells were attached to a set of membranes, at least one membrane was randomly selected and the integrity of its cell monolayer was tested. This provided an approximation of the degree of confluency of the cell monolayer for each of the remaining membranes. To test the integrity of the cell monolayer, the membrane was attached to an electrode and its response to changes in the potassium ion concentration was measured. A low response (change in EMF less than 10% of the change in EMF for the control or "cell free" membrane) was considered indicative of a confluent monolayer of cells on the surface of the membrane. If a low response was observed, the remaining membranes were used in permeability tests (due to a problem with the read-out of the transmitter, the integrity of the cell monolayer was tested but the integrity could not be quantified on 7/12/09).

To perform permeability tests, first the media was removed from the filter house set-up.   In its place, a cytokine mixture was exposed to the cells on the membrane.   The membranes were returned to the incubator for 3 hours. Following 3 hours, the membranes were rinsed with DI water, placed on electrodes, and their response relative to the response of the control or "cell free" membrane was evaluated.

Chapter 5: Discussion

5-1 Results

When faced with hypoxia, a tumor is able to access points of higher oxygen concentration by forming a more extensive network of blood vessels. This process is known as angiogenesis and is responsible for the increased production of VEGF, HGF, bFGF, and TNF-α in the blood stream of individuals with cancer. The purpose of this research was to develop a method using a Caco-2 cell-based biosensor as an indicator for angiogensis by distinguishing between the normal levels of cytokines typical of a healthy individual and elevated levels of cytokines.

As mentioned earlier, there have been many permeability studies performed with the Caco-2 cell line, specifically because of the cells' good absorption properties. The ability of the cells to form a confluent and virtually impenetrable surface on the surface of an ion-selective electrode's membrane was a crucial property to make this research possible. The level of confluency was judged visually by optical microscopy using a 10x lens objective. Figure 5-1 and 5-2 demonstrate the level of confluency achieved 3 and 6 days following seeding the flasks. When the cells were introduced to VEGF, HGF, bFGF, or TNF-α, a disruption to the cell monolayer occurred, resulting in the electrode demonstrating an increased response to the presence of potassium ions.

Figure 5-1: Caco-2 cells 3 days post-seeding (2 cells have been circled)
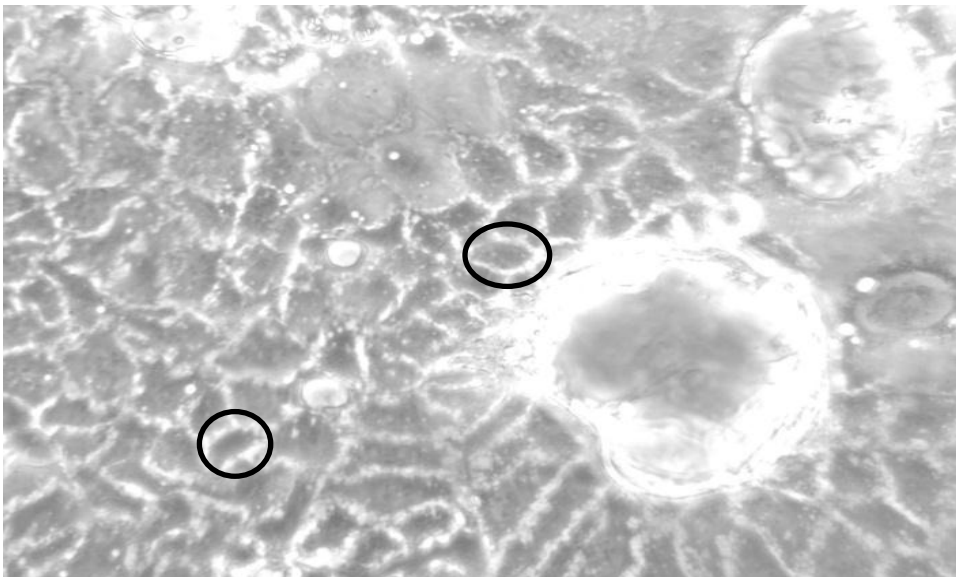
Figure 5-2: Caco-2 cells 6 days post-seeding (2 cells have been circled)

Before testing of the effects of cytokines on the Caco-2 cell-based biosensor could be initiated, the possibility that any observable effects of cytokines on the cell-based biosensor were actually due to effects of the cytokines on the permeability of the membrane itself was excluded. Previous studies with endothelial cell lines have established that when the four cytokines of interest are exposed to the membrane of the electrode, they have no effect on the electrode's response unless cells are present [4]. In other words, any observable difference between the electrode response behavior of the control membranes and the test membranes is attributed to the effects of the cytokines on the cells and not to changes of permeablilty in the polymer membrane itself.

During the planning of the experiment, a decision had to be made as to how long the cytokine exposure time would be for the cells on the membrane. The process of making and preparing the membranes was time-consuming and tedious due to the multi-stepped nature of the process, so a screening test was necessary to avoid wasting time and materials. This was the purpose of the paracellular gap area imaging. This screening test was performed in 24 well plates at a time, allowing for 24 different conditions to be tested in a single pass. This made it possible to test quickly both normal levels as well as elevated levels of all four cytokines as well as test the two potential exposure times of one and three hours. The technique of capturing images under an inverted phase contrast microscope, as well as the method of processing the images, was also quick and easy; allowing the entire screening test to be completed within a day after the cells reached confluency in the well plates. After exposing the cells to

cytokines in a well plate for three hours, a greater disparity in the gaps between the cells was observed with the cells that were exposed to normal levels of cytokines versus elevated levels of cytokines was observed when compared to the one hour exposure time (Figure 5-3 and 5-4). This was especially true in the case of HGF. For this reason, three hours was selected as the exposure time for testing the response of the cells to cytokines after they were grown on the electrode's membrane.
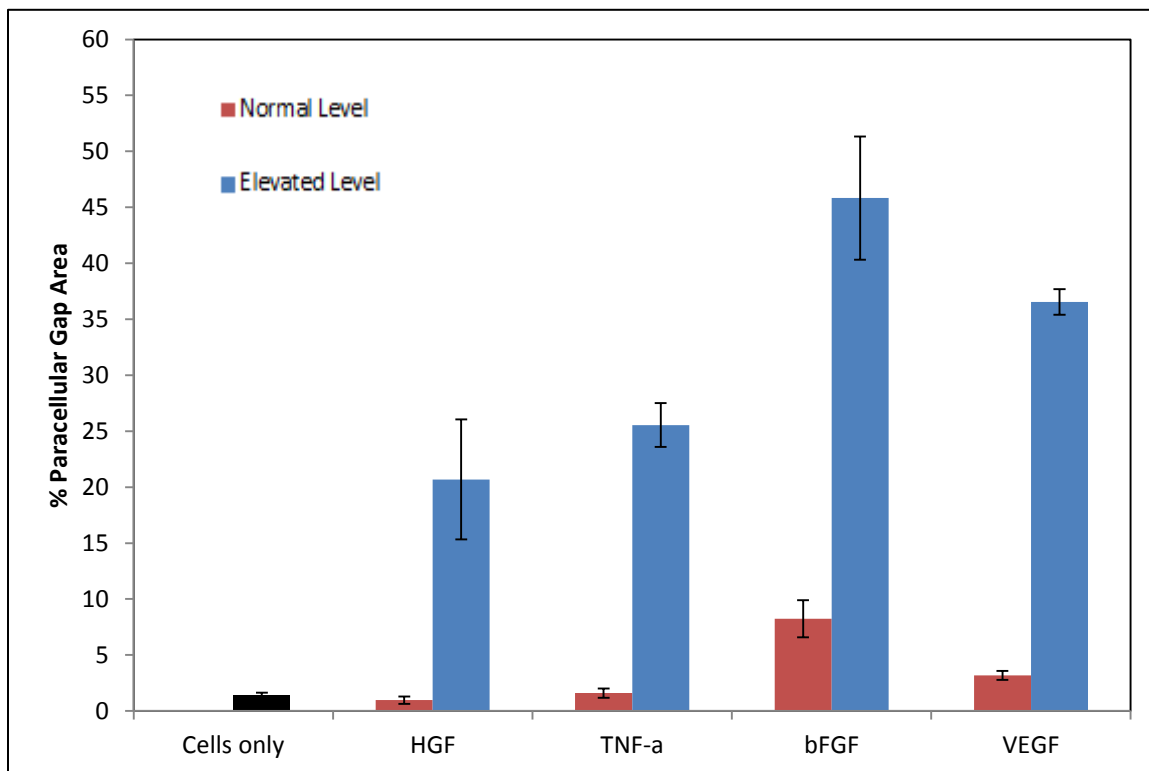
Figure 5-3: Percent paracellular gap area following one hour of exposure to normal levels of cytokines and elevated levels of cytokines (Error bars represent +/- 1 standard deviation N = 12).
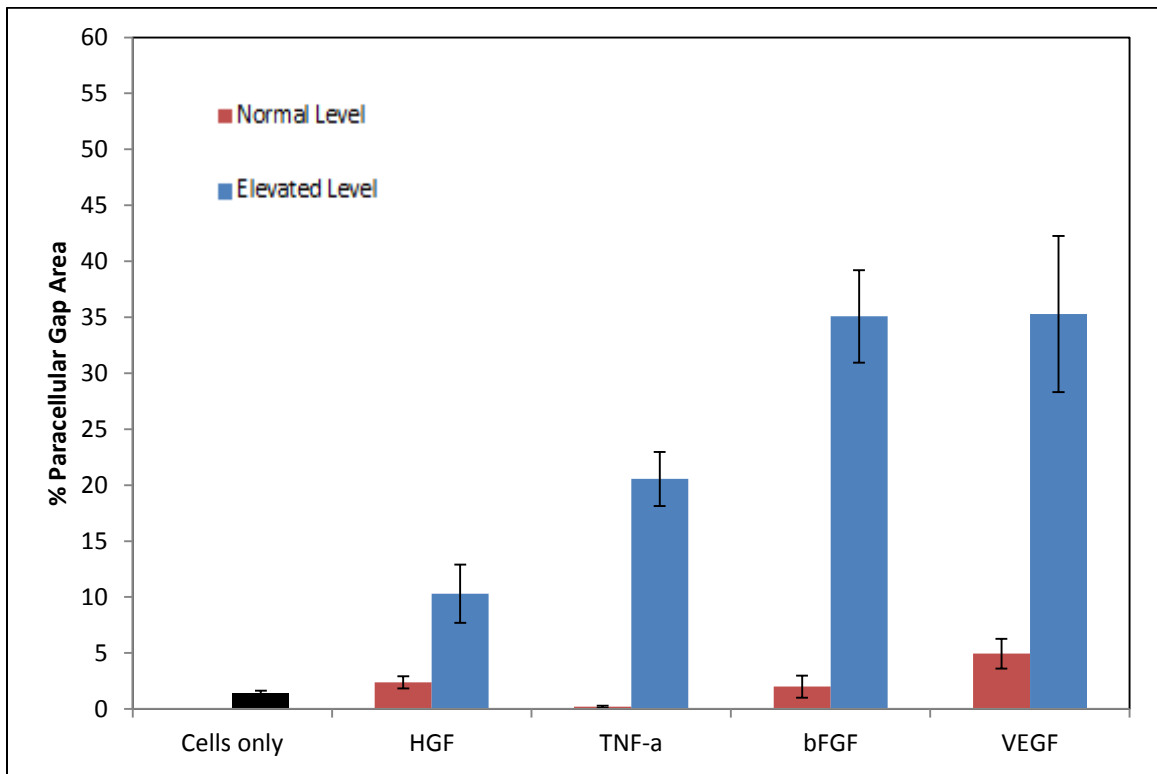
Figure 5-4: Percent paracellular gap area following three hours of exposure to normal levels of cytokines and elevated levels of cytokines (Error bars represent +/- 1 standard deviation N = 12).

The paracellular gap area test was a good indication of how the electrodes would respond to cytokines and therefore it was a useful screening tool.

Figures 5-5 through 5-13 demonstrates the electrode response data that was collected for cell-attached membranes not exposed to cytokine mixture (i.e. "Cells Only"), for cell-attached membranes exposed to normal and elevated levels of each cytokine for 3 hours, and for the corresponding membrane each membrane section corresponds to that was neither cell-attached nor exposed to cytokine mixture (i.e. "Control").

Following a three hour exposure to the cytokine solutions, a significant difference in electrode response between the cells that were exposed to a low concentration of cytokines and the cells that were exposed to a high concentration of cytokines was observed (Figure 5-14). Table 5-1 summarizes the test results of all membrane sections that were used and tested during the generation of the data in the electrode experiment.
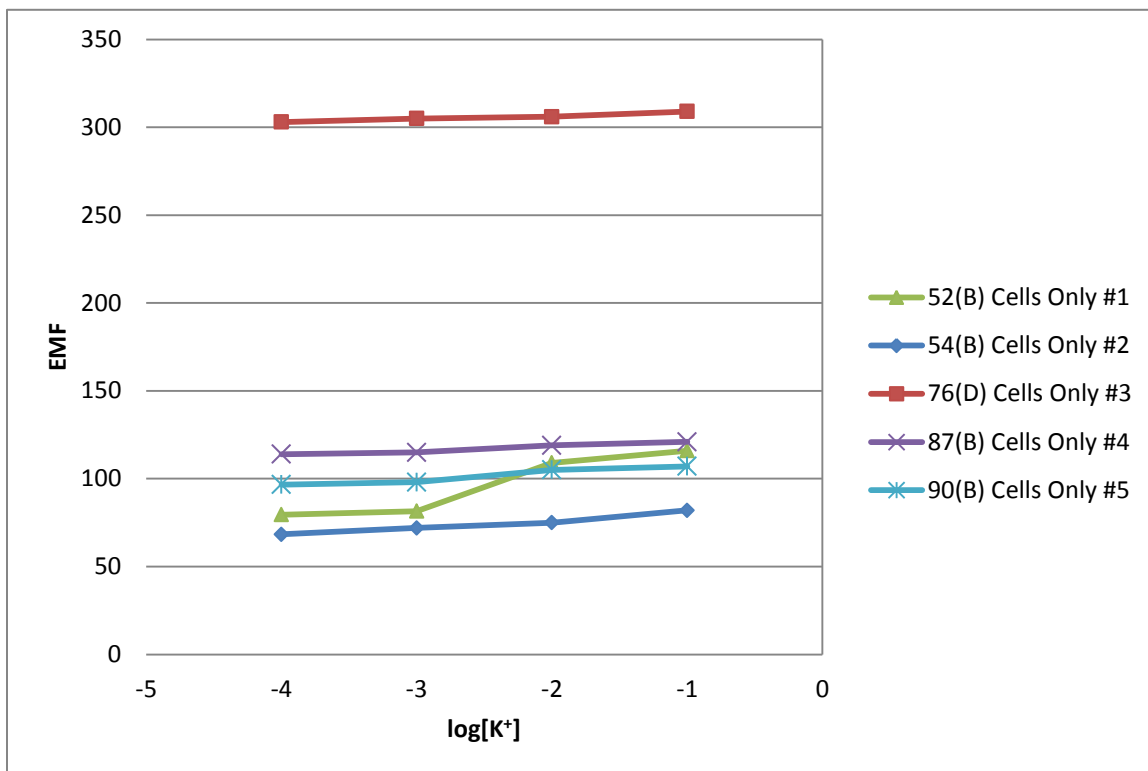
Figure 5-5: Electrode response data for cell-attached membranes not exposed to cytokine mixture (i.e. "Cells Only")
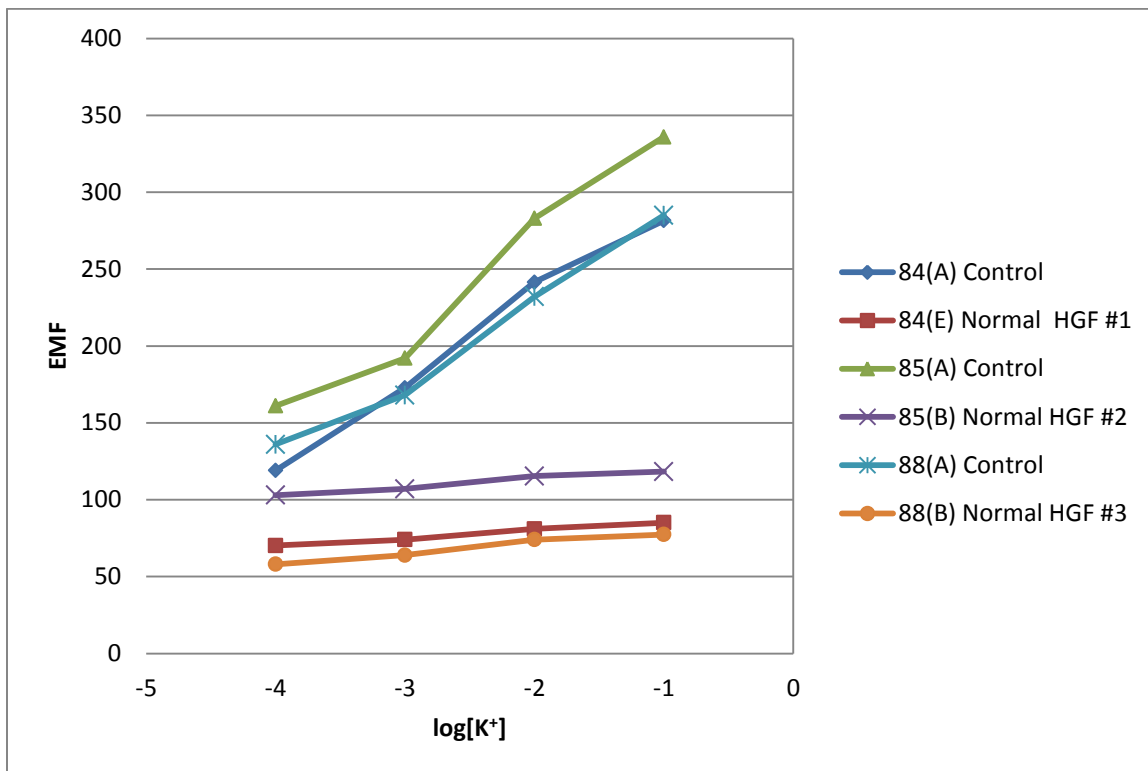
Figure 5-6: Electrode response data for cell-attached membranes exposed to a normal level of HGF for 3 hours as well as for the corresponding membrane each membrane section corresponds to that was neither cell-attached nor exposed to cytokine mixture (i.e. "Control")
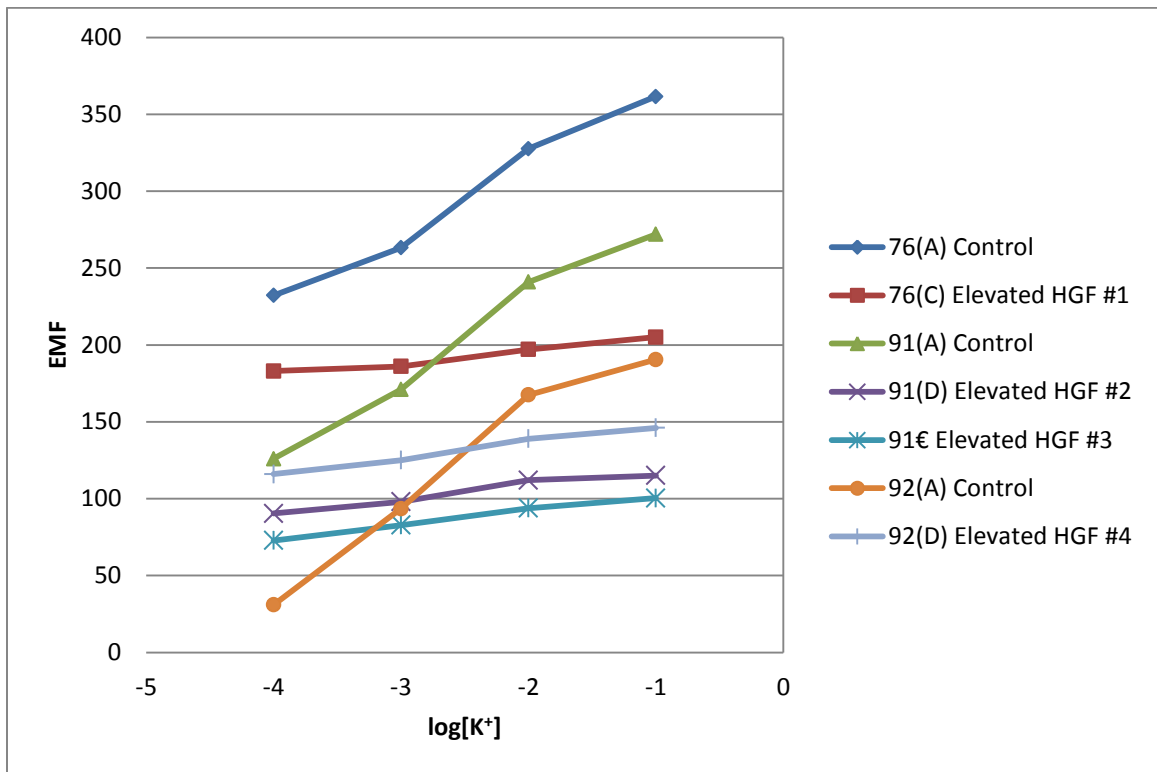
Figure 5-7: Electrode response data for cell-attached membranes exposed to an elevated level of HGF for 3 hours as well as for the corresponding membrane each membrane section corresponds to that was neither cell-attached nor exposed to cytokine mixture (i.e. "Control")
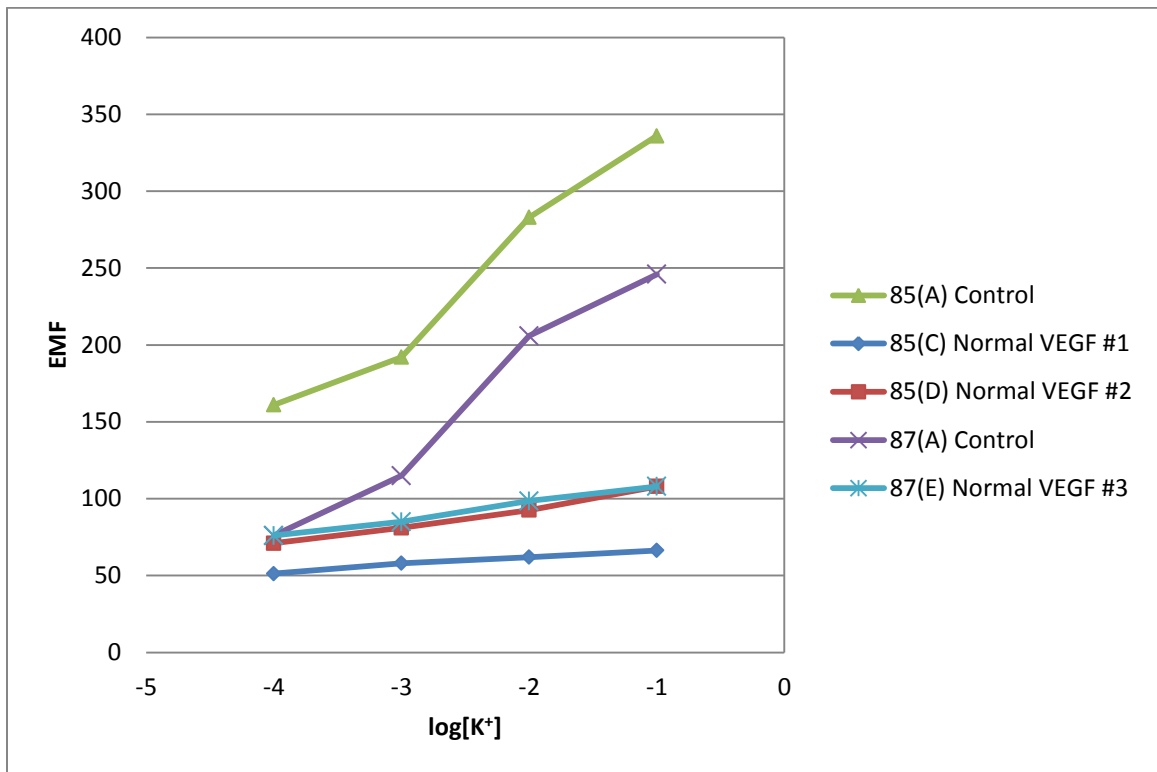
Figure 5-8: Electrode response data for cell-attached membranes exposed to a normal level of VEGF for 3 hours as well as for the corresponding membrane each membrane section corresponds to that was neither cell-attached nor exposed to cytokine mixture (i.e. "Control")
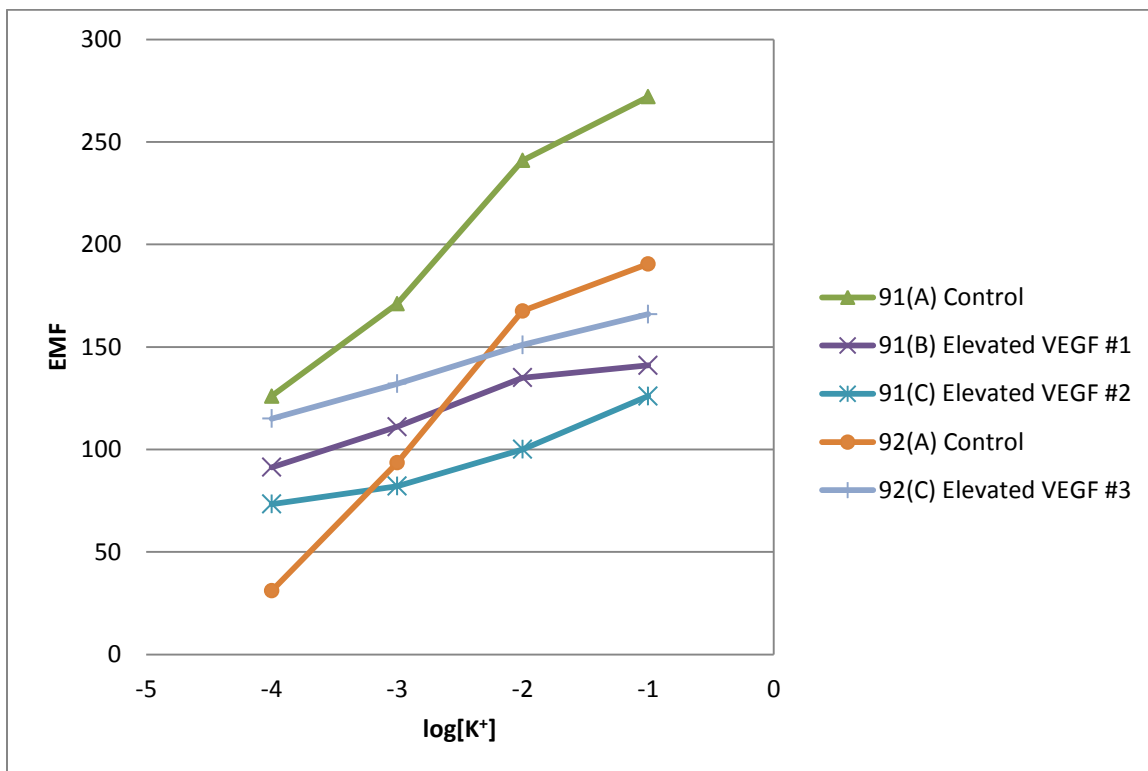
Figure 5-9: Electrode response data for cell-attached membranes exposed to an elevated level of VEGF for 3 hours as well as for the corresponding membrane each membrane section corresponds to that was neither cell-attached nor exposed to cytokine mixture (i.e. "Control")
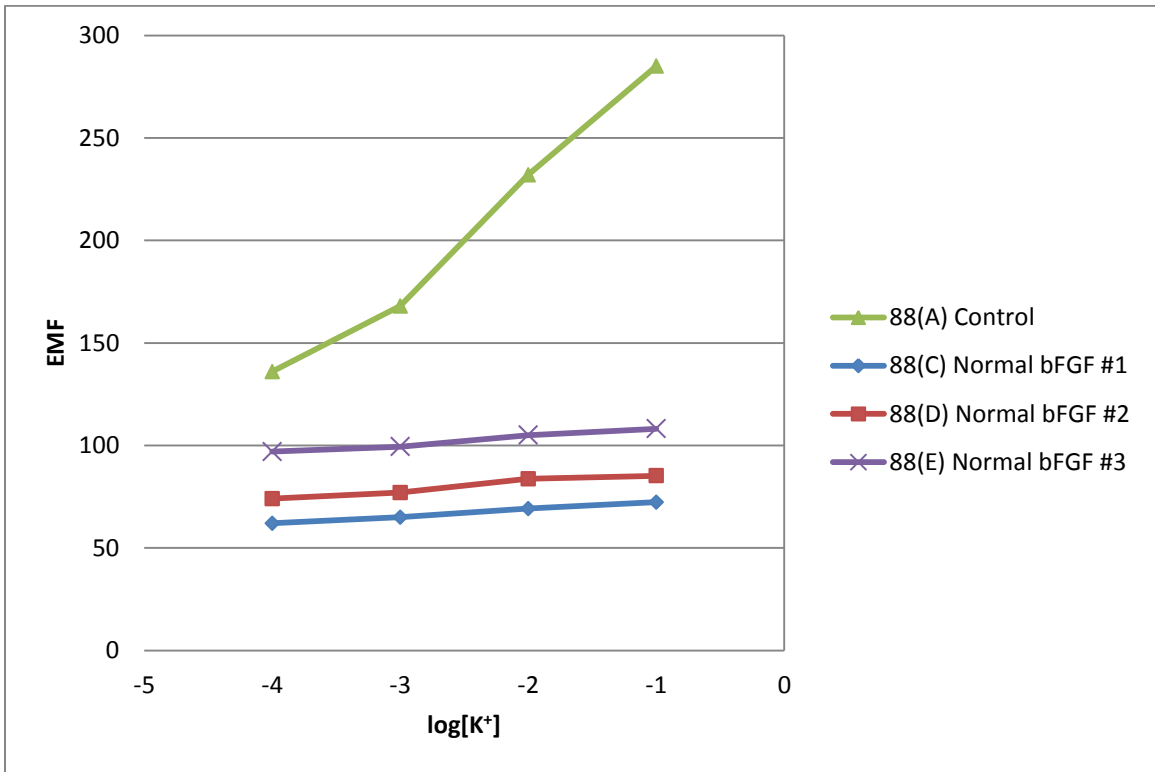
Figure 5-10: Electrode response data for cell-attached membranes exposed to a normal level of bFGF for 3 hours as well as for the corresponding membrane each membrane section corresponds to that was neither cell-attached nor exposed to cytokine mixture (i.e. "Control")
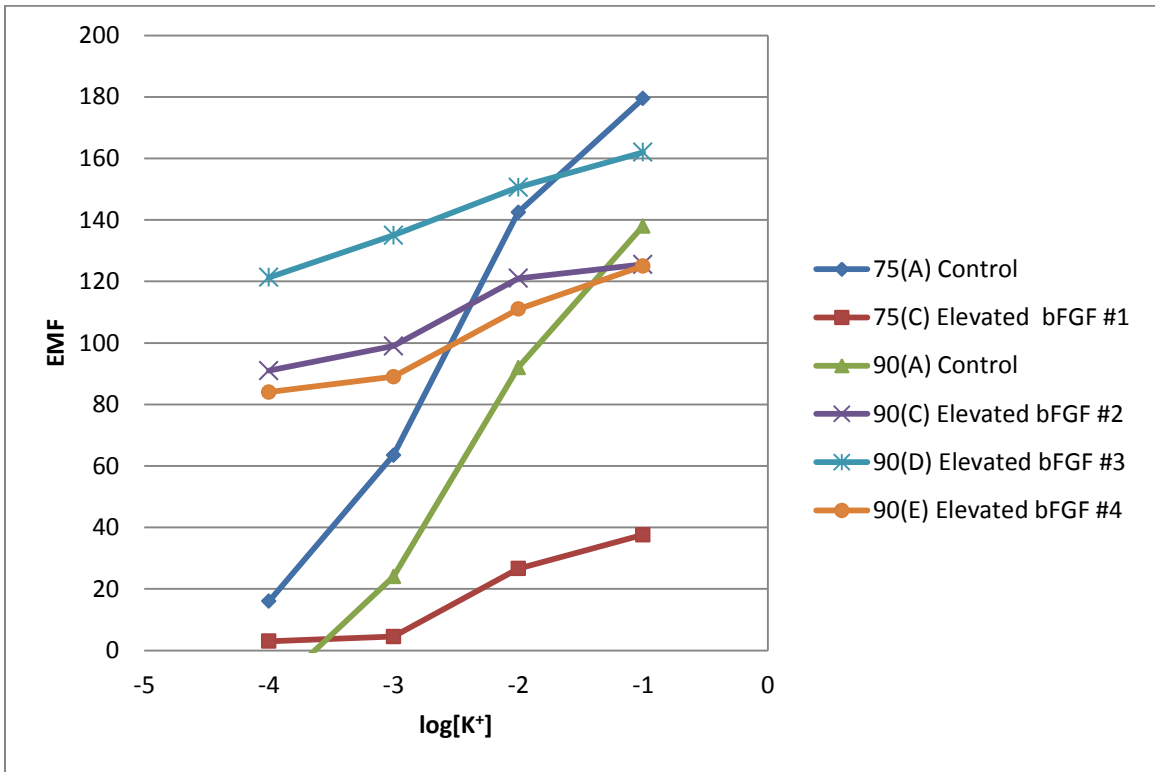
Figure 5-11: Electrode response data for cell-attached membranes exposed to an elevated level of bFGF for 3 hours as well as for the corresponding membrane each membrane section corresponds to that was neither cell-attached nor exposed to cytokine mixture (i.e. "Control")
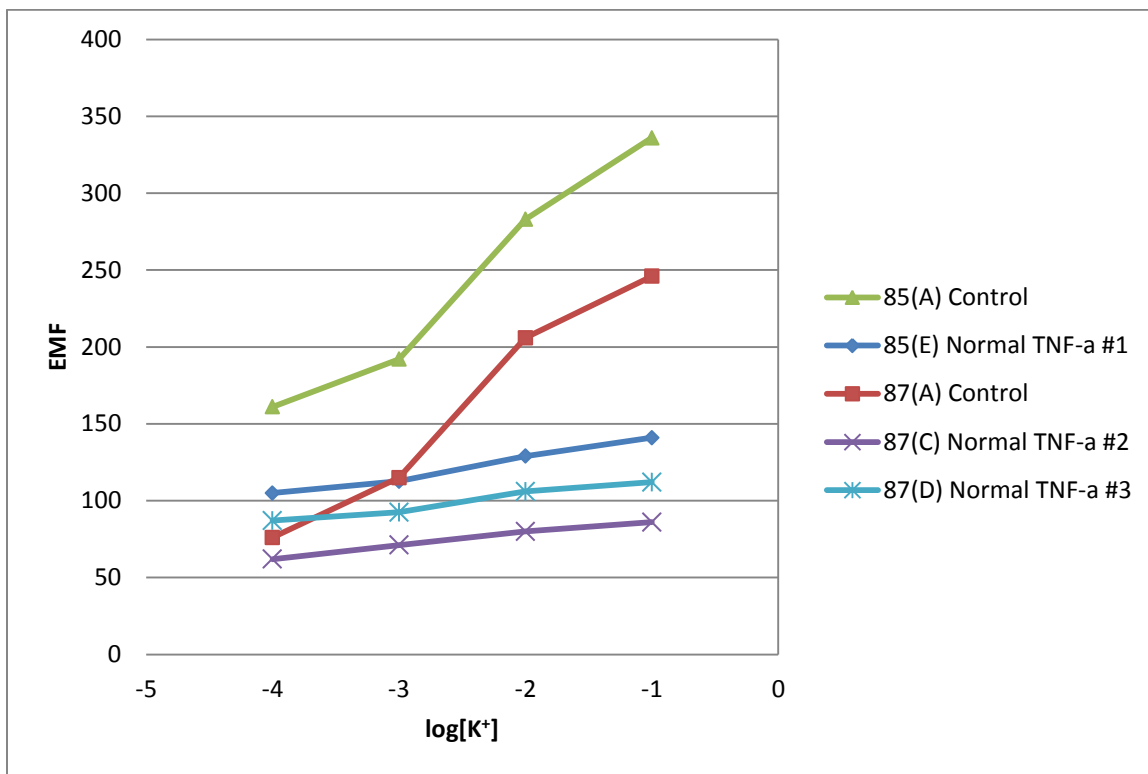
Figure 5-12: Electrode response data for cell-attached membranes exposed to a normal level of TNF-α for 3 hours as well as for the corresponding membrane each membrane section corresponds to that was neither cell-attached nor exposed to cytokine mixture (i.e. "Control")
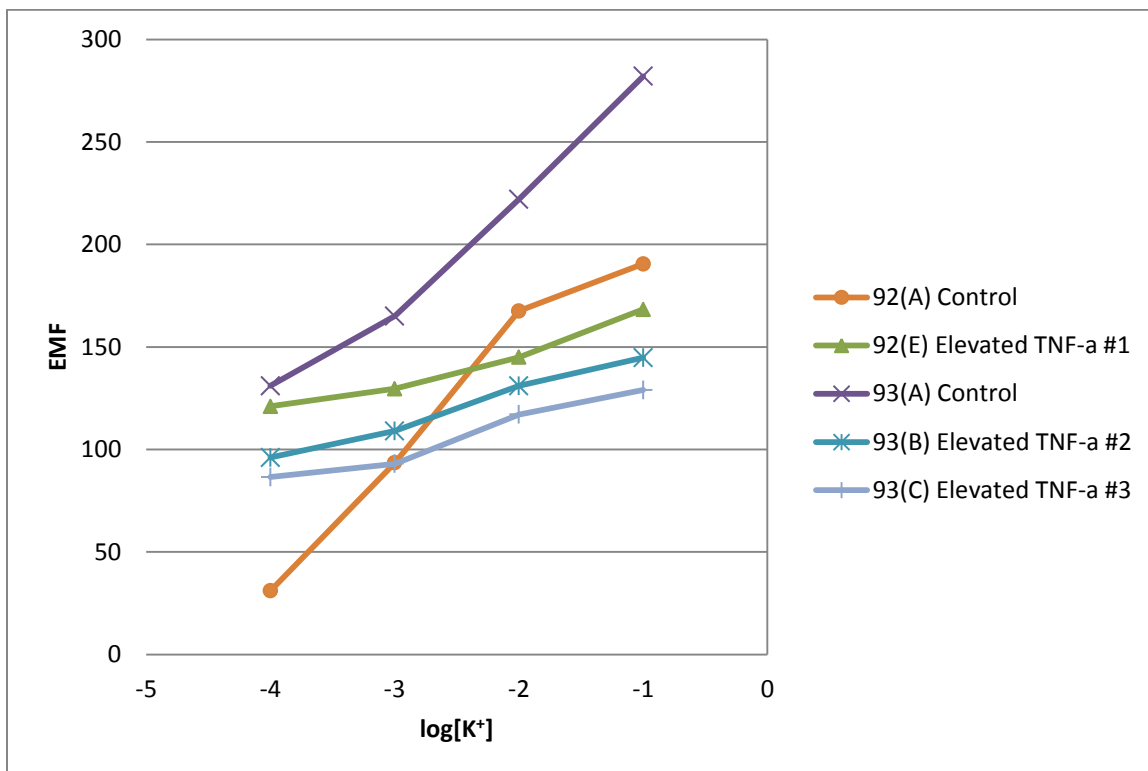
Figure 5-13: Electrode response data for cell-attached membranes exposed to an elevated level of TNF-α for 3 hours as well as for the corresponding membrane each membrane section corresponds to that was neither cell-attached nor exposed to cytokine mixture (i.e. "Control")
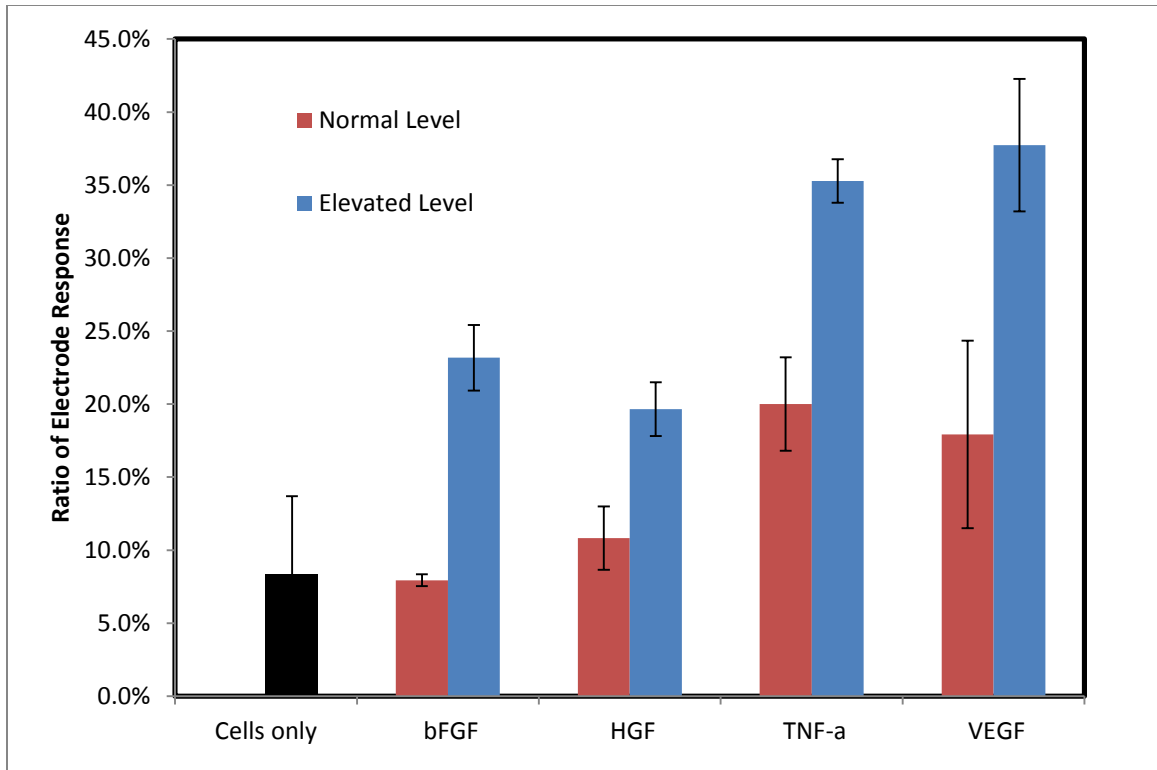
Figure 5-14: Electrode response ratio following three hours of exposure to a normal level of cytokines and an elevated level of cytokines (Error bars represent +/- 1 standard deviation N = 5 for "Cells only", N = 4 for Elevated Levels of bFGF and HGF, N = 3 otherwise).

Table 5-1: Summary of Membranes Used and Data Collected

| Date	Membrane	Electrode Response Slope	R^2	Conditions
6/3/2008	52(A)	54.91	1.00	Control
6/5/2008	54(A)	55.47	0.97	Control
6/29/2008	52(B)	13.7	0.89	Cells only
6/29/2008	54(B)	4.41	0.96	Cells only
2/21/2009	75(A)	56.95	0.98	Control
3/22/2009	75(C)	12.59	0.92	Elevated bFGF #1
3/22/2009	76(D)	1.90	0.96	Cells only
4/8/2009	84(A)	55.62	0.99	Control
4/8/2009	85(A)	61.6	0.97	Control
4/8/2009	87(A)	60.07	0.97	Control
4/8/2009	88(A)	51.1	0.98	Control
7/12/2009	84(E)	5.17	0.99	Normal hGF #1
7/12/2009	85(B)	5.43	0.97	Normal hGF #2
7/12/2009	85(C)	4.9	0.98	Normal VEGF #1
7/12/2009	85(D)	12.26	0.99	Normal VEGF #2
7/12/2009	85(E)	12.44	0.98	Normal TNF-α #1
7/19/2009	87(B)	2.5	0.95	Cells only
7/19/2009	87(C)	8.09	0.99	Normal TNF-α #2
7/19/2009	87(D)	8.85	0.97	Normal TNF-α #3
7/19/2009	87(E)	10.95	0.99	Normal VEGF #3
7/19/2009	88(B)	6.82	0.97	Normal hGF #3
7/19/2009	88(C)	3.51	1.00	Normal bFGF #1
7/19/2009	88(D)	4.03	0.95	Normal bFGF #2
7/19/2009	88(E)	3.89	0.98	Normal bFGF #3
8/2/2009	90(A)	52.4	0.99	Control
8/2/2009	91(A)	50.8	0.98	Control
8/2/2009	92(A)	55.25	0.96	Control
8/2/2009	93(A)	51	0.99	Control
9/13/2009	90(B)	3.79	0.92	Cells only
9/13/2009	90(C)	12.55	0.94	Elevated bFGF #2
9/13/2009	90(D)	13.77	1.00	Elevated bFGF #3
9/13/2009	90(E)	14.5	0.95	Elevated bFGF #4
9/13/2009	91(B)	17.31	0.95	Elevated VEGF #1
9/13/2009	91(C)	17.6	0.95	Elevated VEGF #2
9/13/2009	91(D)	8.78	0.95	Elevated hGF #1
9/13/2009	91(E)	9.38	0.99	Elevated hGF #2
9/27/2009	92(B)	2.44	0.96	Cells only
9/27/2009	92(C)	17.2	1.00	Elevated VEGF #3
9/27/2009	92(D)	10.4	0.99	Elevated hGF #3
9/27/2009	92(E)	15.73	0.96	Elevated TNF-α #1
9/27/2009	93(B)	16.81	0.99	Elevated TNF-α #2
9/27/2009	93(C)	15.15	0.96	Elevated TNF-α #3

In both the gap area test and the electrode test, there was a clear difference between the cells that were exposed to a low level of cytokines and the cells that were exposed to a high level of cytokines. Although results from the gap area study suggested that of all of the four cytokines, bFGF played the most significant role in increasing the spaces between the epithelial cells, both TNF-α and VEGF had a greater impact on the cell-to-cell adhesion when tested on the electrode. Although this may be due to the crude nature of the gap area method and interpretation of results, a second explanation is that the permeability of the cells in controlled by transcelluar pathways in addition to paracellular pathways. One possibility for the discrepancy between the changes in permeability seen in percent paracellular gap area calculations and the electrode response measurements could be due to the possibility that the percent paracellular gap area calculations only take into account changes in the paracellular pathways and not changes in the transcellular pathways. On the other hand, the electrode measurements may be affected by changes in both paracellular and transcellular pathways. The notion that solutes may travel through the cells and between the gaps in the cell monolayer could also explain why there were only small gaps between the cells that were not exposed to cytokines but still demonstrated a notable response to potassium ions on the electrode. There were some inconsistencies in how much resistance the membranes with cells that were not exposed to cytokines demonstrated. Although this resulted in cell-only membranes with responses higher than the

established standard, the subsequent results were saved because cell-based membranes exposed to the elevated levels of cytokines still maintained a much higher response in comparison.

5-2 Future Work

Some improvements may be made to decrease the waste of time and materials in the membrane fabrication process, improve the inhibition of response for the cell-only control membrane-based biosensors, possibly reduce the standard error of the repeats and better understand the mechanisms involved with the permeability changes. Future work may include:

- Investigating better membrane fabrication methods

- Altering the culture conditions

- Utilizing other epithelial cell lines

- Exploring the mechanisms of permeability changes in cells

5-2.1 Investigating better membrane fabrication methods

During the period between December 2007 and August 2009, over 90 membranes were fabricated. Of those membranes that were tested, 24 performed well enough to be used in further tests. The result was a waste in time and resources and it would be useful to solve this problem before further related experiments are undertaken. Several alterations to the fabrication method have been tested with limited success. For example, while working on the membrane fabrication in a separate lab a switch in the anionic-repelling salt from KTpClB (potassium tetrakis (p-chlorophenyl) borate) to KTTFPB was made due to the improved solubility in chloroform of the latter. Although still

unexplained, this adjustment to the membrane's composition seemed to help with the performance and the change was adopted permanently starting in May 2008.

5-2.2 Altering the culture conditions

It is important to consider the variation in performance of Caco-2 cells due to laboratory conditions. In these experiments a narrow range of passage was used (21-33), the same seeding cell density was used, the same media composition was used, the substrate was the same, and the period of time allowed for the cells to attach, spread, and organize remained constant (3 days). It may be of interest to consider the cell-based biosensor performance when other cell culture parameters are used. A different range of cell passage number may result in, for example, better cell monolayer confluency upon seeding on the electrode membrane and thus more inhibition in the response of the control biosensor. As discussed earlier, other types of media and substrates exist that may result in more rapid maturation and differentiation of a confluent cell monolayer. If it is not possible to quicken the cell maturation, then one should consider an increase in the duration of time allotted for cell maturation to occur, being aware that a potential trade-off exists as the polymer membrane leaches active ingredients into the aqueous culture media with time.

5-2.3 Utilizing other epithelial cell lines

Other epithelial cell lines have been used to study the permeability of particular solutes as well as the effects of permeability-altering substances. Some examples include T84, MDCK, and LLC-PK1.

T84, like Caco-2, is a human adenocarcinoma cell line that has been well tested for its permeability properties but differs from Caco-2 in that it can form fully differentiated monolayers with 5 to 10 days post-seeding [60]. MDCK and LLC-PK1 can form monolayers ready for tests after three to six days of culturing, although MDCK generally demonstrates lower TEER values than Caco-2 cells and LLC-PK1 tends to absorb greater amounts of commonly tested compounds [61-63].

5-2.4 Exploring the mechanisms of permeability changes in cells

As previously mentioned, it is possible that some of the differences observed between the paracellular gap area screening method and the electrode test method could involve whether the pathway employed was paracellular or transcellular. For verification of what pathways are being used to cause the changes in cell permeability of the cell-based biosensors, a study could be done. In another experiment [64] it was discovered that if p38 mitogen-activated protein kinase (p38 MAPK) was blocked with an inhibitor, SB203580, then cytomix was unable to disrupt the barrier function of Caco-2 cells in its usual manner. Since p38 MAPK mediates the cell-to-cell junctions of epithelial cells [65], using this particular inhibitor could render the cytokines ineffective at causing permeability

changes at these junctions of the cells. Any observed changes in electrode

response would thus be indicative of a change in transcellular permeability.

List of Abbreviations

ATCC	American Type Culture Collection
bFGF	Basic Fibroblast Growth Factor
CDI	Carbonyldiimidazole
CTA	Cellulose Triacetate
DMSO	Dimethyl sulfoxide
EDTA	Ethylenediaminetetraacetic Acid
EMF	Electromotive Force
F-actin	Filamentous Actin
FBS	Fetal Bovine Serum
GRGDS	Glycine-Arginine-Glycine-Aspartic Acid-Serine
HGF	Hepatocyte Growth Factor
HIF-1	Hypoxia-Inducible Factor
HUVECs	Human Umbilical-Vein Endothelial Cells
KCl	Potassium Chloride
KTpClB	Potassium Tetrakis (p-Chlorophenyl) Borate
KTTFPB	Tetrakis[3,5-bis(trifluoromethyl)phenyl]boron potassium
MDCK	Madin-Darby Canine Kidney
NaOH	Sodium Hydroxide
NF-kB	Nuclear Factor Kappa B
NPOE	2-Nitrophenyl Octyl Ether
p38 MAPK	p38 Mitogen-Activated Protein Kinase
PBS	Phosphate Buffered Saline Solution
PFA	Paraformaldehyde
P-gp	P-glycoprotein
PVC	Polyvinyl Chloride
pVHL	Von Hippel-Lindau Protein
RGD	Arginine-Glycine-Aspartic Acid
TNF-α	Tumor Necrosis Factor Alpha
TEER	Transepithelial Resistance
Tg	Glass Transition Temperature
TIFF	Tagged Image File Format
VEGF	Vascular Endothelial Growth Factor
VHL	Von Hippel-Lindau

References

1. May, K.M.L., et al., *Development of a whole-cell-based biosensor for detecting histamine as a model toxin.* Analytical Chemistry, 2004. **76**(14): p. 4156-4161.

2. Ghosh, G., L.G. Bachas, and K.W. Anderson, *Biosensor incorporating cell barrier architectures for detecting Staphylococcus aureus alpha toxin.* Analytical and Bioanalytical Chemistry, 2007. **387**(2): p. 567-574.

3. May, K.M.L., et al., *Vascular endothelial growth factor as a biomarker for the early detection of cancer using a whole cell-based biosensor.* Analytical and Bioanalytical Chemistry, 2005. **382**(4): p. 1010-1016.

4. Ghosh, G., et al., *Measuring permeability with a whole cell-based biosensor as an alternate assay for angiogenesis: Comparison with common in vitro assays.* Biosensors & Bioelectronics, 2008. **23**(7): p. 1109-1116.

5. Ghosh, G., L.G. Bachas, and K.W. Anderson, *Biosensor incorporating cell barrier architectures on ion selective electrodes for early screening of cancer.* Analytical and Bioanalytical Chemistry, 2008. **391**(8): p. 2783-2791.

6. Rundle, C.C. *A Beginners Guide to Ion-Selective Electrode Measurements.* 2000 June 5, 2008 September 7, 2008].

7. Buck, R.P. and E. Lindner, *RECOMMENDATIONS FOR NOMENCLATURE OF ION-SELECTIVE ELECTRODES - (IUPAC RECOMMENDATIONS 1994).* Pure and Applied Chemistry, 1994. **66**(12): p. 2527-2536.

8. Eggins, B.R., *Chemical Sensors and Biosensors*2002: John Wiley and Sons.

9. Harsányi, G., *Polymer Films in Sensor Applications*1995: CRC Press.

10. Bakker, E., P. Buhlmann, and E. Pretsch, *Carrier-based ion-selective electrodes and bulk optodes. 1. General characteristics.* Chemical Reviews, 1997. **97**(8): p. 3083-3132.

11. Lee, K.S., et al., *ASYMMETRIC CARBONATE ION-SELECTIVE CELLULOSE-ACETATE MEMBRANE ELECTRODES WITH REDUCED SALICYLATE INTERFERENCE.* Analytical Chemistry, 1993. **65**(21): p. 3151-3155.

12. Brooks, H.A., et al., *Effect of surface-attached heparin on the response of potassium-selective electrodes.* Analytical Chemistry, 1996. **68**(8): p. 1439-1443.

13. Buhlmann, P., E. Pretsch, and E. Bakker, *Carrier-based ion-selective electrodes and bulk optodes. 2. Ionophores for potentiometric and optical sensors.* Chemical Reviews, 1998. **98**(4): p. 1593-1687.

14. Rose, L. and A.T.A. Jenkins, *The effect of the ionophore valinomycin on biomimetic solid supported lipid DPPTE/EPC membranes.* Bioelectrochemistry, 2007. **70**(2): p. 387-393.

15. Atwood, J.L. and J.W. Steed, *Encyclopedia of Supramolecular Chemistry*, ed. C. Press2004.

16. Boulton, A.A., G.B. Baker, and W. Walz, *The Neuronal Microenvironment*1988: Humana Press.

17. Johnson, R.D. and L.G. Bachas, *Ionophore-based ion-selective potentiometric and optical sensors.* Analytical and Bioanalytical Chemistry, 2003. **376**(3): p. 328-341.

18. Behrens, I. and T. Kissel, *Do cell culture conditions influence the carrier-mediated transport of peptides in Caco-2 cell monolayers?* European Journal of Pharmaceutical Sciences, 2003. **19**(5): p. 433-442.

19. Pageot, L.P., et al., *Human cell models to study small intestinal functions: Recapitulation of the crypt-villus axis.* Microscopy Research and Technique, 2000. **49**(4): p. 394-406.

20. Pinto, M., et al., *ENTEROCYTE-LIKE DIFFERENTIATION AND POLARIZATION OF THE HUMAN-COLON CARCINOMA CELL-LINE CACO-2 IN CULTURE.* Biology of the Cell, 1983. **47**(3): p. 323-330.

21.   Grasset, E., et al., *EPITHELIAL PROPERTIES OF HUMAN COLONIC-CARCINOMA CELL-LINE CACO-2 - ELECTRICAL PARAMETERS.* American Journal of Physiology, 1984. **247**(3): p. C260-C267.

22.   D'Souza, V.M., et al., *High glucose concentration in isotonic media alters Caco-2 cell permeability.* Aaps Pharmsci, 2003. **5**(3): p. 9.

23.   Shim, S.M. and H. Kwon, *ASSESSING ABSORBABILITY OF BIOACTIVE COMPONENTS IN ALOE USING IN VITRO DIGESTION MODEL WITH HUMAN INTESTINAL CELL.* Journal of Food Biochemistry. **34**(2): p. 425-438.

24.   Wang, Y., et al., *Stereoselective Transport and Uptake of Propranolol Across Human Intestinal Caco-2 Cell Monolayers.* Chirality. **22**(3): p. 361-368.

25.   Fisher, S.J., P.W. Swaan, and N.D. Eddington, *The Ethanol Metabolite Acetaldehyde Increases Paracellular Drug Permeability In Vitro and Oral Bioavailability In Vivo.* Journal of Pharmacology and Experimental Therapeutics. **332**(1): p. 326-333.

26.   Chong, S.H., S.A. Dando, and R.A. Morrison, *Evaluation of Biocoat (R) intestinal epithelium differentiation environment (3-day cultured Caco-2 cells) as an absorption screening model with improved productivity.* Pharmaceutical Research, 1997. **14**(12): p. 1835-1837.

27.   BriskeAnderson, M.J., J.W. Finley, and S.M. Newman, *The influence of culture time and passage number on the morphological and physiological development of Caco-2 cells.* Proceedings of the Society for Experimental Biology and Medicine, 1997. **214**(3): p. 248-257.

28.   Balimane, P.V., Y.H. Han, and S.H. Chong, *Current industrial practices of assessing permeability and P-glycoprotein interaction.* Aaps Journal, 2006. **8**(1): p. E1-E13.

29.   Avdeef, A., *Leakiness and Size Exclusion of Paracellular Channels in Cultured Epithelial Cell Monolayers-Interlaboratory Comparison.* Pharmaceutical Research. **27**(3): p. 480-489.

30.   Yang, L., et al., *Physicochemical and Biological Characterization of Monoketocholic Acid, a Novel Permeability Enhancer.* Molecular Pharmaceutics, 2009. **6**(2): p. 448-456.

31.   Korjamo, T., et al., *Effect of N-betainate and N-piperazine derivatives of chitosan on the paracellular transport of mannitol in Caco-2 cells.* European Journal of Pharmaceutical Sciences, 2008. **35**(3): p. 226-234.

32.   Lim, S.L. and L.Y. Lim, *Effects of citrus fruit juices on cytotoxicity and drug transport pathways of Caco-2 cell monolayers.* International Journal of Pharmaceutics, 2006. **307**(1): p. 42-50.

33.   Liang, E., et al., *Permeability measurement of macromolecules and assessment of mucosal antigen sampling using in vitro converted M cells.* Journal of Pharmacological and Toxicological Methods, 2001. **46**(2): p. 93-101.

34.   Gao, Y., et al., *Improvement of intestinal absorption of insulin and water-soluble macromolecular compounds by chitosan oligomers in rats.* International Journal of Pharmaceutics, 2008. **359**(1-2): p. 70-78.

35.   Maher, S., et al., *Melittin as an epithelial permeability enhancer I: Investigation of its mechanism of action in Caco-2 monolayers.* Pharmaceutical Research, 2007. **24**(7): p. 1336-1345.

36.   Neuhaus, W., et al., *A novel tool to characterize paracellular transport: The APTS-Dextran ladder.* Pharmaceutical Research, 2006. **23**(7): p. 1491-1501.

37.   *Methods in Enzymology*, ed. V.L.C. John N. Abelson, Melvin I. Simon. Vol. Bacterial Pathogenesis, Part B: Interaction of Pathogenic Bacteria with Host Cells, Volume 236 Academic Press.

38.   Lando, D., et al., *Oxygen-dependent regulation of hypoxia-inducible factors by prolyl and asparaginyl hydroxylation.* European Journal of Biochemistry, 2003. **270**(5): p. 781-790.

39.   Semenza, G.L., *Targeting HIF-1 for cancer therapy.* Nature Reviews Cancer, 2003. **3**(10): p. 721-732.

40.   Hara, S., et al., *Hypoxia enhances c-Met/HGF receptor expression and signaling by activating HIF-1 alpha in human salivary gland cancer cells.* Oral Oncology, 2006. **42**(6): p. 593-598.

41.   Bos, R., et al., *Hypoxia-inducible factor-1 alpha is associated with angiogenesis, and expression of bFGF, PDGF-BB, and EGFR in invasive breast cancer.* Histopathology, 2005. **46**(1): p. 31-36.

42.   Koong, A.C., E.Y. Chen, and A.J. Giaccia, *HYPOXIA CAUSES THE ACTIVATION OF NUCLEAR FACTOR KAPPA-B THROUGH THE PHOSPHORYLATION OF I-KAPPA-B-ALPHA ON TYROSINE RESIDUES.* Cancer Research, 1994. **54**(6): p. 1425-1430.

43.   Chandel, N.S., et al., *Role of oxidants in NF-kappa B activation and TNF-alpha gene transcription induced by hypoxia and endotoxin.* Journal of Immunology, 2000. **165**(2): p. 1013-1021.

44.   Heer, K., et al., *Serum vascular endothelial growth factor in breast cancer: Its relation with cancer type and estrogen receptor status.* Clinical Cancer Research, 2001. **7**(11): p. 3491-3494.

45.   Dirix, L.Y., et al., *Elevated levels of the angiogenic cytokines basic fibroblast growth factor and vascular endothelial growth factor in sera of cancer patients.* British Journal of Cancer, 1997. **76**(2): p. 238-243.

46.   Premkumar, V.G., et al., *Serum cytokine levels of interleukin-1 beta, -6, -8, tumour necrosis factor-alpha and vascular endothelial growth factor in breast cancer patients treated with tamoxifen and supplemented with co-enzyme Q(10), riboflavin and niacin.* Basic & Clinical Pharmacology & Toxicology, 2007. **100**(6): p. 387-391.

47.   Cronauer, M.V., et al., *Basic fibroblast growth factor levels in cancer cells and in sera of patients suffering from proliferative disorders of the prostate.* Prostate, 1997. **31**(4): p. 223-233.

48.   Sheen-Chen, S.M., et al., *Serum levels of hepatocyte growth factor in patients with breast cancer.* Cancer Epidemiology Biomarkers & Prevention, 2005. **14**(3): p. 715-717.

49.   Wong, V. and B.M. Gumbiner, *A synthetic peptide corresponding to the extracellular domain of occludin perturbs the tight junction permeability barrier.* Journal of Cell Biology, 1997. **136**(2): p. 399-409.

50.   McCarthy, K.M., et al., *Occludin is a functional component of the tight junction.* Journal of Cell Science, 1996. **109**: p. 2287-2298.

51.   Behrens, J., et al., *Loss of Epithelial Differentiation and Gain of Invasiveness Correlates with Tyrosine Phosphorylation of the E-Cadherin Beta-Catenin Complex in Cells Transformed with a Temperature-Sensitive V-SRC Gene.* Journal of Cell Biology, 1993. **120**(3): p. 757-766.

52.   Sommers, C.L., et al., *Alterations in Beta-Catenin Phosphorylation and Plakoglobin Expression in Human Breast-Cancer Cells.* Cancer Research, 1994. **54**(13): p. 3544-3552.

53.   Volberg, T., et al., *The Effect of Tyrosine-Specific Protein-Phosphorylation on the Assembly of Adherens-Type Junctions.* Embo Journal, 1992. **11**(5): p. 1733-1742.

54.   Pasdar, M., et al., *Inhibition of junction assembly in cultured epithelial cells by hepatocyte growth factor scatter factor is concomitant with increased stability and altered phosphorylation of the soluble junctional molecules.* Cell Growth & Differentiation, 1997. **8**(4): p. 451-462.

55.   Cui, W., et al., *Tumor necrosis factor alpha increases epithelial barrier permeability by disrupting tight junctions in Caco-2 cells.* Brazilian Journal of Medical and Biological Research. **43**(4): p. 330-337.

56.   Suarez, S. and K. Ballmer-Hofer, *VEGF transiently disrupts gap junctional communication in endothelial cells.* Journal of Cell Science, 2001. **114**(6): p. 1229-1235.

57.   Wu, J.C., et al., *JNK signaling pathway is required for bFGF-mediated surface cadherin downregulation on HUVEC.* Experimental Cell Research, 2008. **314**(3): p. 421-429.

58.   Ghosh, G., "A WHOLE CELL BASED BIOSENSOR FOR MONITORING PHYSIOLOGICAL TOXINS AND EARLY SCREENING OF CANCER" (2008). *Doctoral Dissertations.* Paper 578.

59.   Geldhof, A.B., et al., *Morphometric analysis of cytolysis in cultured cell monolayers: A simple and versatile method for the evaluation of the cytotoxic activity and the fate of LAK cells.* Laboratory Investigation, 2002. **82**(1): p. 105-107.

60.   Mochizuki, T., et al., *Transepithelial Transport of Macromolecular Substances in IL-4 Treated Human Intestinal T84 Cell Monolayers.* Bioscience Biotechnology and Biochemistry, 2009. **73**(11): p. 2422-2426.

61.   Bohets, H., et al., *Strategies for Absorption Screening in Drug Discovery and Development.* Current Topics in Medicinal Chemistry, 2001. **1**(5): p. 367-383.

62.   Takaai, M., et al., *Pharmacokinetic analysis of transcellular transport of levofloxacin across LLC-PK1 and Caco-2 cell monolayers.* Biological & Pharmaceutical Bulletin, 2007. **30**(11): p. 2167-2172.

63.   Weinstein, K., et al., *Cultured epithelial cell assays used to estimate intestinal absorption potential.* Pharmaceutical Profiling in Drug Discovery and Lead Selection, ed. K.E. Borchardt RT, Lipinski CA, Thakker DR, Wang B2004, Arlington, VA: AAPS Press. 217-234.

64.   Wang, Q., et al., *Cytokine-induced epithelial permeability changes are regulated by the activation of the p38 mitogen-activated protein kinase pathway in cultured Caco-2 cells.* Shock, 2008. **29**(4): p. 531-537.

65.   Cohen, T.S., et al., *MAPk Activation Modulates Permeability of Isolated Rat Alveolar Epithelial Cell Monolayers Following Cyclic Stretch.* Plos One. **5**(4): p. 9.

Vita

Christina Nicole Simmons

Born	*Owensboro, KY*	*January 24, 1982*

Education

B.A. Degree in Chemistry
University of Kentucky, *Lexington, KY*
Minored in Mathematics; graduated cum
laude with 3.4 G.P.A.

2005

B.S. Degree in Biology
University of Kentucky, *Lexington, KY*

2004

Career History

Research Associate, *DSM Nutritional
Products -- Martek*

2009-Present

Engineering Technologist, *Analysts
International*

2006-2007

Chemical Technician Specialist,
Analysts International

2005-2006